AEOS Astrophysique Extragalactique et Observations Spatiales

The optical gravitational lens experiment and discovery of multiply imaged quasars with Gaia

Jean Surdej

(Ludovic Delchambre, François Finet, Olivier Wertz, Priyanka Jalan)

20 November 2019,
IUCAA (Pune, India)

"All different philosophical, economic and political systems that govern men just agree on one point: let's fool them…"

Roger Waters
(Pink Floyd, 1974)

Quiz

$$v = \frac{c}{n}$$

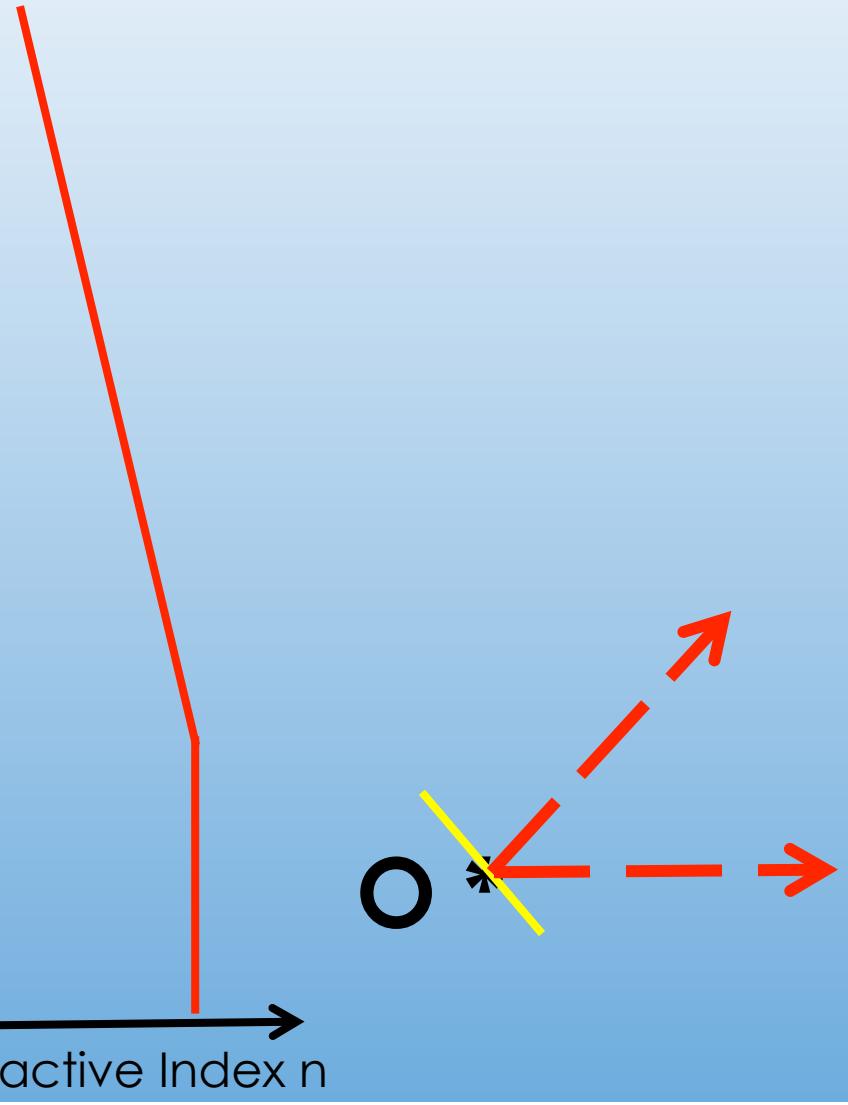

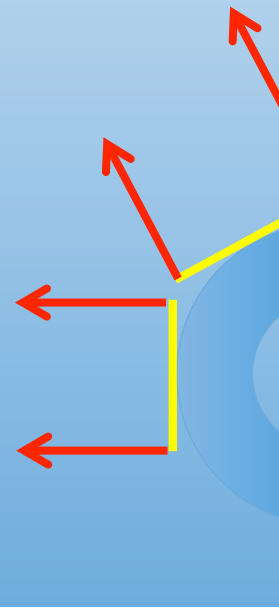

$$n = 1 - \frac{2U}{c^2}$$

$$v = \frac{c}{n}$$

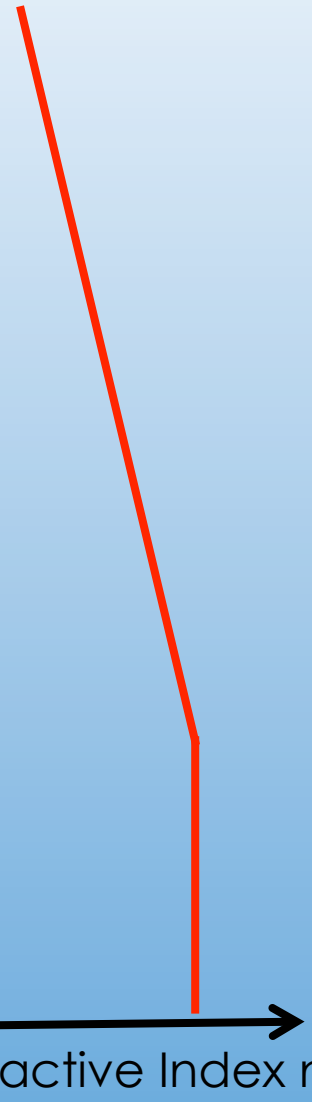

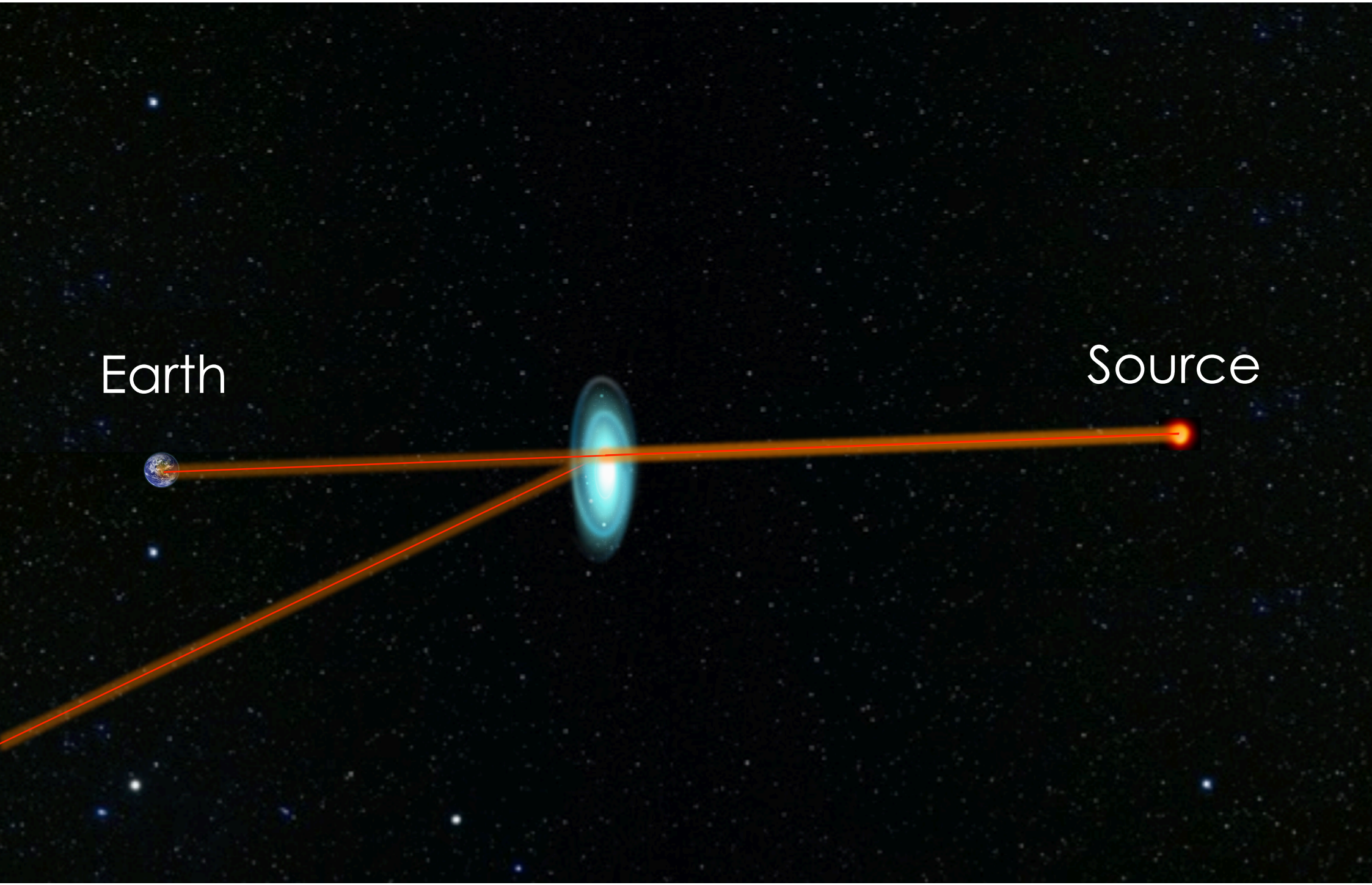
Earth
Source

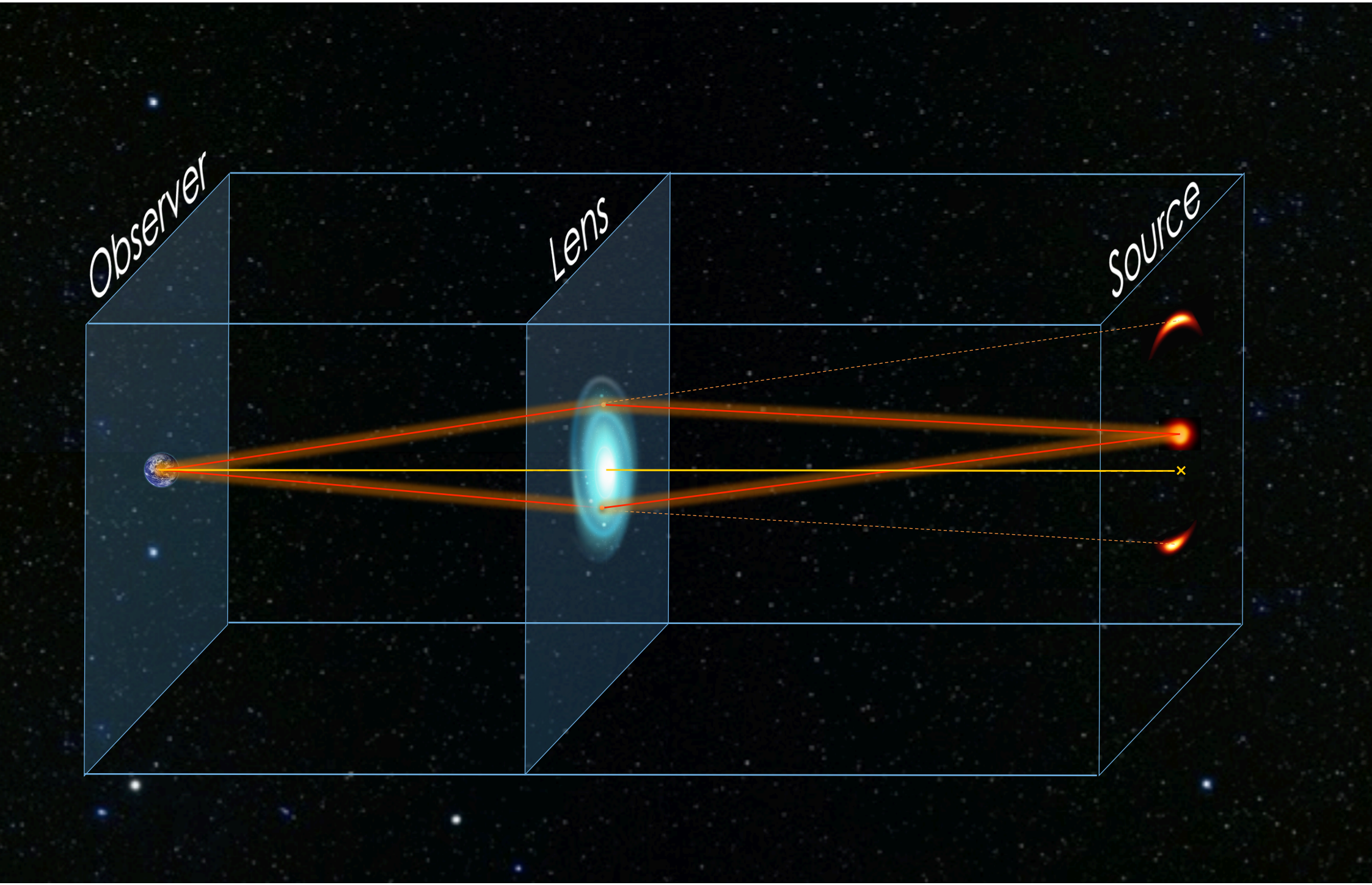
Observer
Lens
Source

Sjur Refsdal (1964)

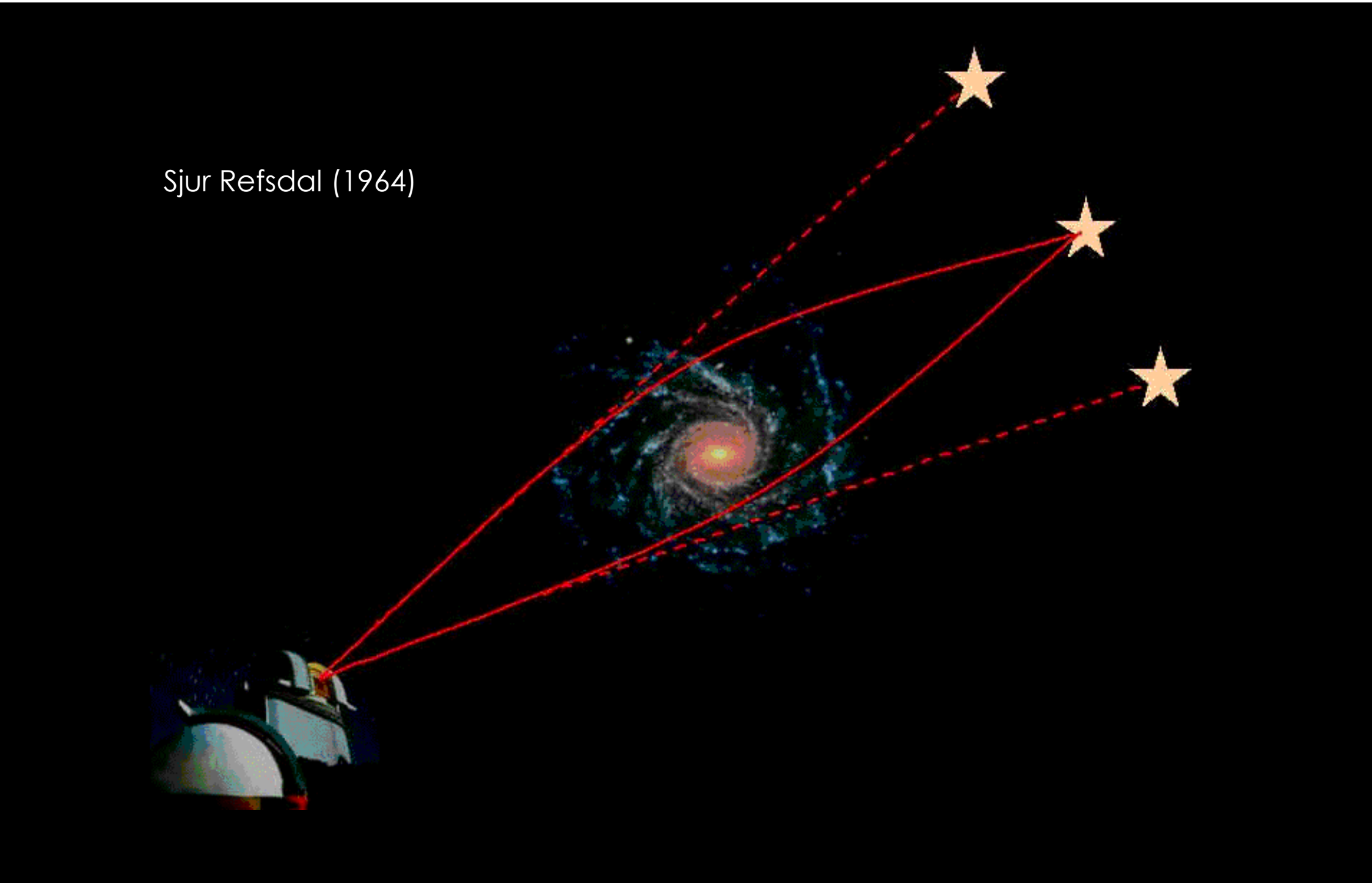

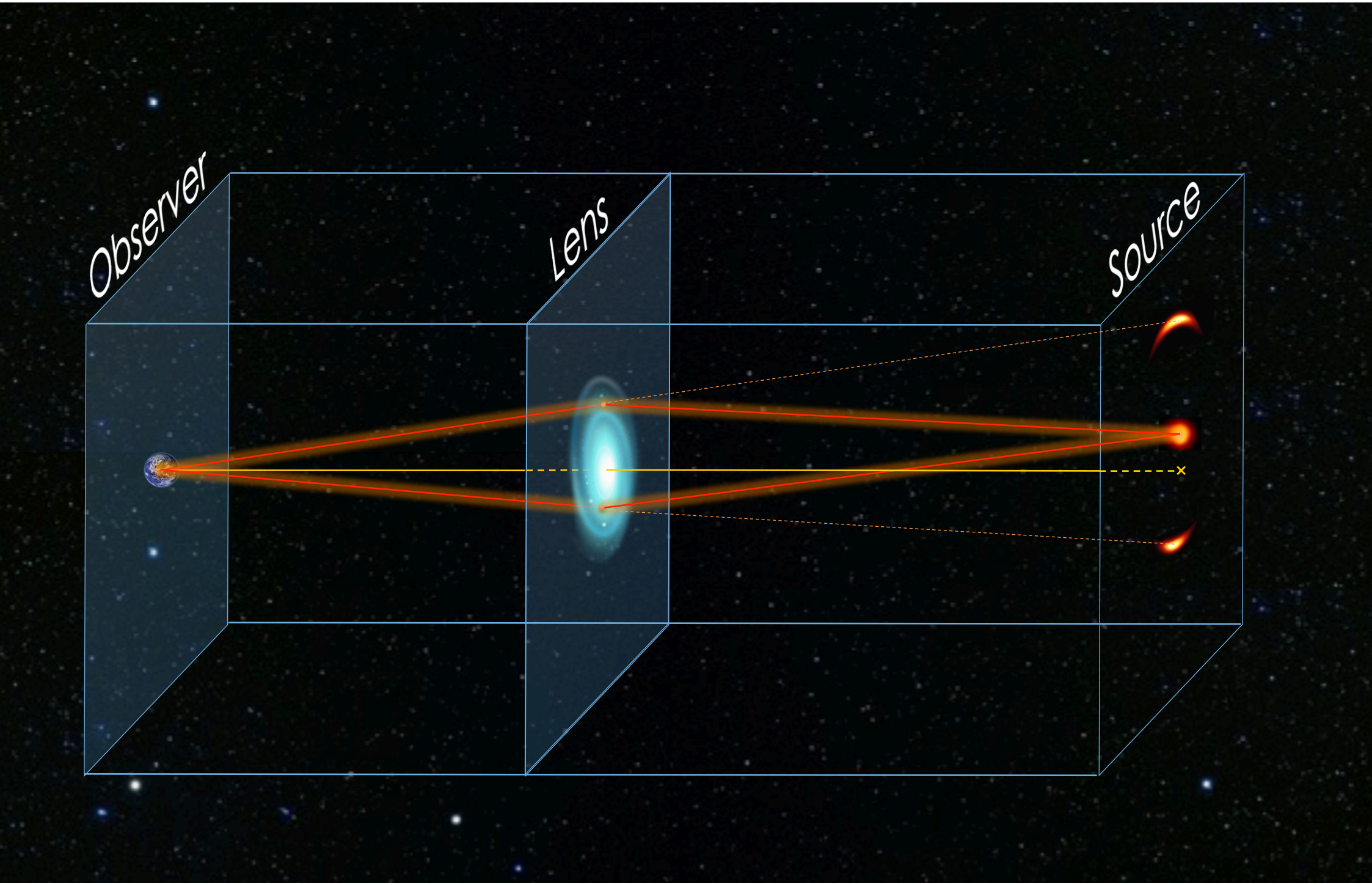
Observer
Lens
Source

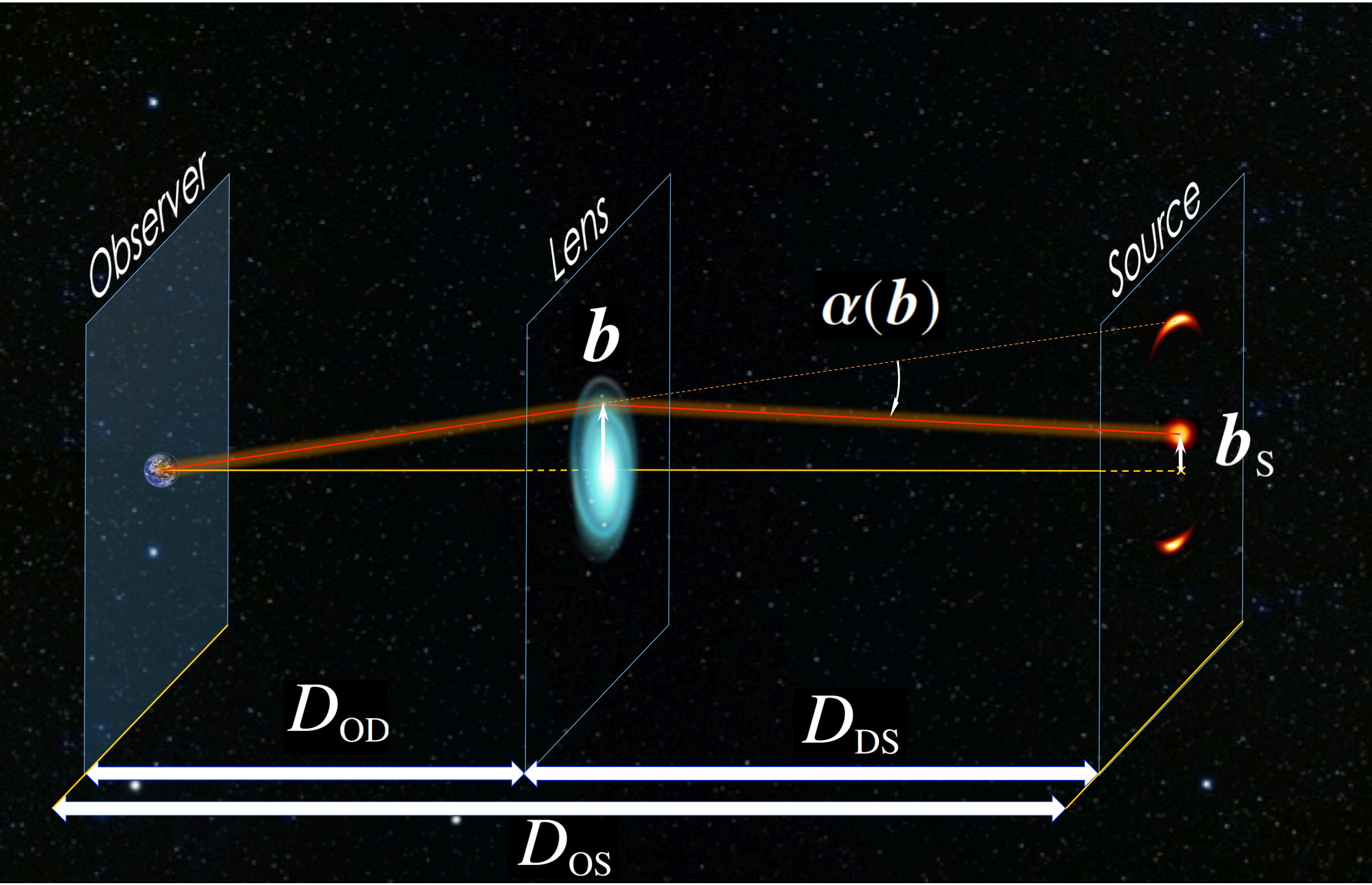
Observer
Lens
Source
b
α(b)
b_S
D_OD
D_DS
D_OS

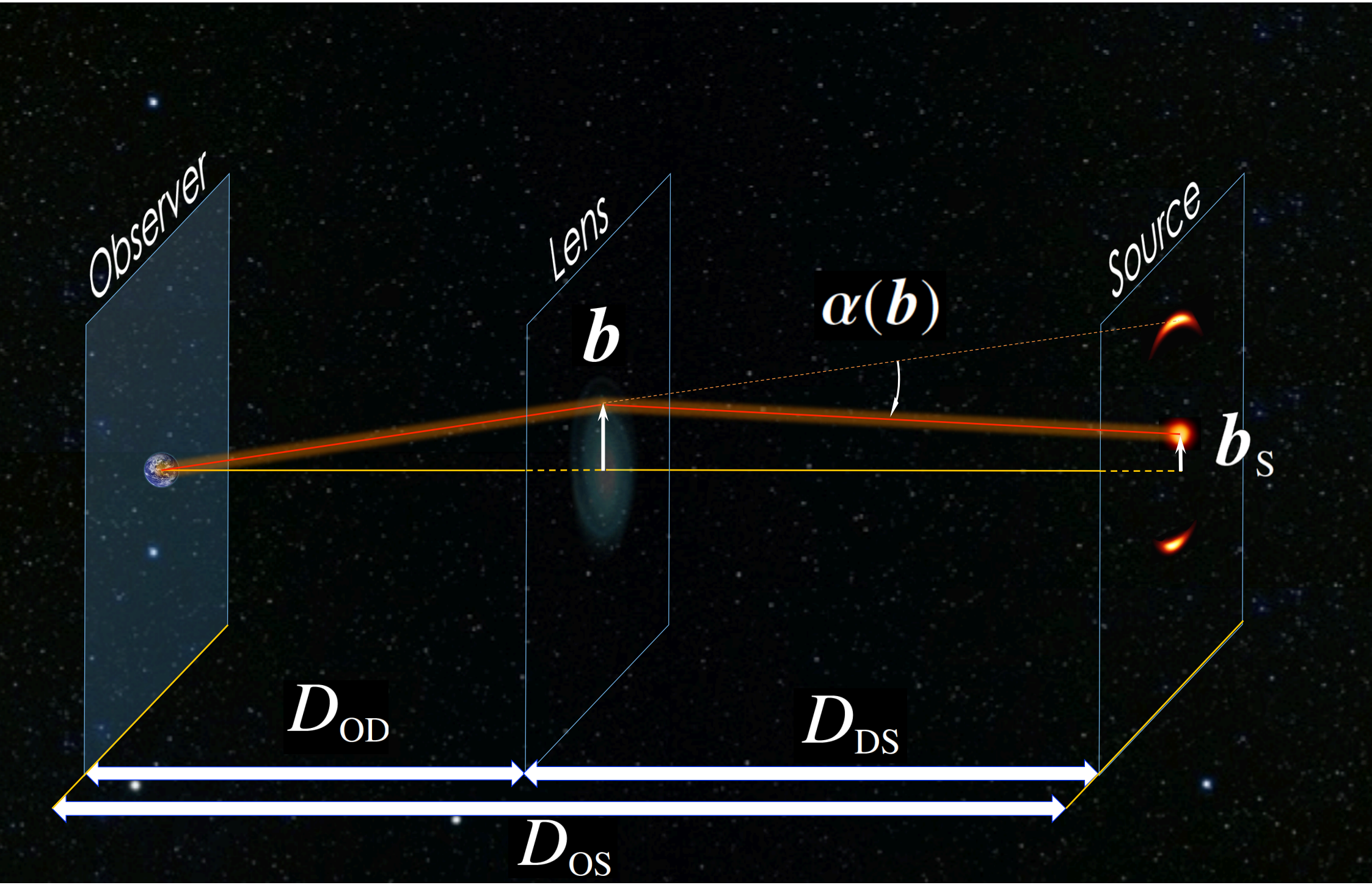
Observer
Lens
Source
b
α(b)
b_S
D_OD
D_DS
D_OS

The lens equation

$$\boldsymbol{b} = \frac{D_{OD}}{D_{OS}}\,\boldsymbol{\alpha}(\boldsymbol{b}) + \frac{D_{DS}}{D_{OS}}\,\boldsymbol{b}_S$$

The lens equation

$$\boldsymbol{b}_{\mathrm{S}} = \frac{D_{\mathrm{OS}}}{D_{\mathrm{OD}}}\,\boldsymbol{b} + D_{\mathrm{DS}}\,\boldsymbol{\alpha}(\boldsymbol{b})$$

The lens equation

$$\boldsymbol{b}_{\mathrm{S}} = \frac{D_{\mathrm{OS}}}{D_{\mathrm{OD}}}\,\boldsymbol{b} + D_{\mathrm{DS}}\,\boldsymbol{\alpha}(\boldsymbol{b})$$

1 The lens equation

$$\boldsymbol{b}_S = \frac{D_{OS}}{D_{OD}}\,\boldsymbol{b} + D_{DS}\,\boldsymbol{\alpha}(\boldsymbol{b})$$

$$\frac{D_{OD}}{D_{OS}}\frac{\boldsymbol{b}_S}{b_0} = \frac{\boldsymbol{b}}{b_0} + \frac{D_{OD}\,D_{DS}}{b_0\,D_{OS}}\,\boldsymbol{\alpha}(\boldsymbol{b})$$

1 The lens equation

$$\boldsymbol{y} = \boldsymbol{x} + \hat{\boldsymbol{\alpha}}(\boldsymbol{x})$$

$$\frac{D_{\mathrm{OD}}}{D_{\mathrm{OS}}}\frac{\boldsymbol{b}_{\mathrm{S}}}{b_0} = \frac{\boldsymbol{b}}{b_0} + \frac{D_{\mathrm{OD}}D_{\mathrm{DS}}}{b_0 D_{\mathrm{OS}}}\boldsymbol{\alpha}(\boldsymbol{b})$$

$$\boldsymbol{y} = \frac{D_{\mathrm{OD}}}{D_{\mathrm{OS}}}\frac{\boldsymbol{b}_{\mathrm{S}}}{b_0} \qquad \boldsymbol{x} = \frac{\boldsymbol{b}}{b_0} \qquad \hat{\boldsymbol{\alpha}}(\boldsymbol{x}) = \frac{D_{\mathrm{OD}}D_{\mathrm{DS}}}{b_0 D_{\mathrm{OS}}}\boldsymbol{\alpha}(\boldsymbol{b})$$

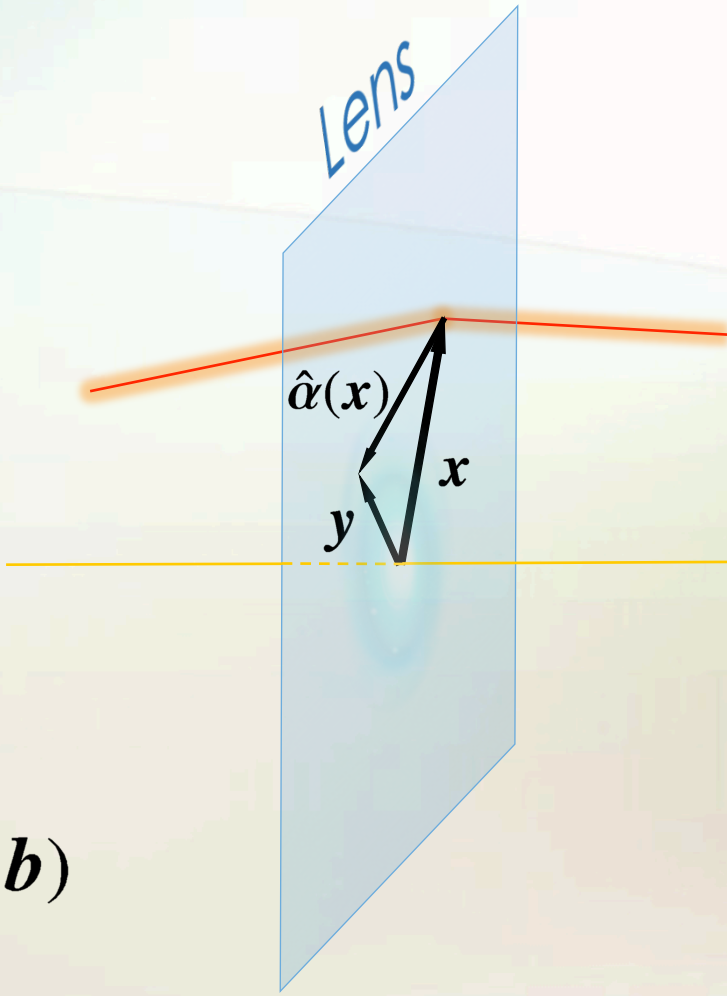

1 The adimensional lens equation

$$\boldsymbol{y} = \boldsymbol{x} + \hat{\boldsymbol{\alpha}}(\boldsymbol{x})$$

$$\hat{\boldsymbol{\alpha}}(\boldsymbol{x}) = -\frac{1}{\pi}\iint_{\mathbb{R}^2} \kappa(\boldsymbol{x}')\,\frac{\boldsymbol{x}-\boldsymbol{x}'}{|\boldsymbol{x}-\boldsymbol{x}'|^2}\,\mathrm{d}\boldsymbol{x}'$$

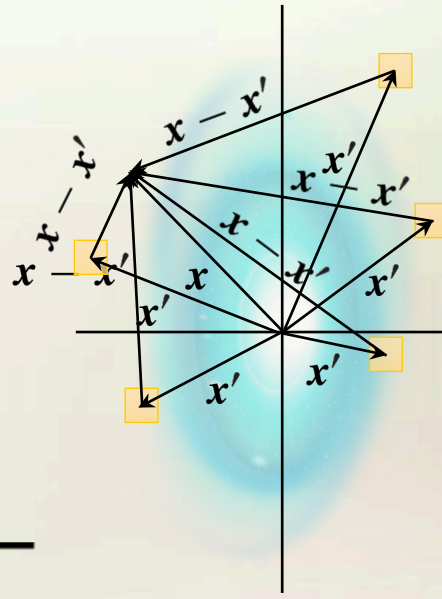

$$= \frac{\Sigma(b_0\boldsymbol{x})}{\Sigma_{\mathrm{cr}}} \quad \text{where} \quad \Sigma_{\mathrm{cr}} = \frac{c^2}{4\pi G}\,\frac{D_{\mathrm{OS}}}{D_{\mathrm{DS}}\,D_{\mathrm{OD}}}$$

1 The adimensional lens equation

$$\boldsymbol{y} = \boldsymbol{x} + \hat{\boldsymbol{\alpha}}(\boldsymbol{x})$$

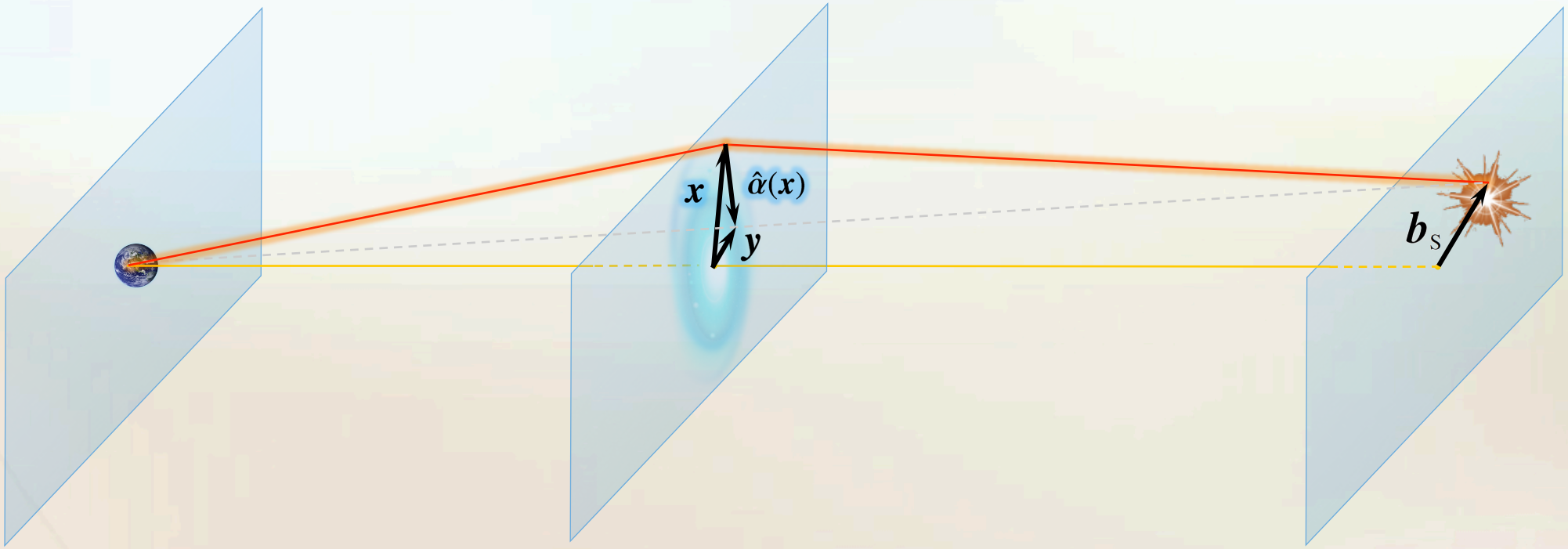

1 The adimensional lens equation

$$\boldsymbol{y} = \boldsymbol{x} + \hat{\boldsymbol{\alpha}}(\boldsymbol{x})$$

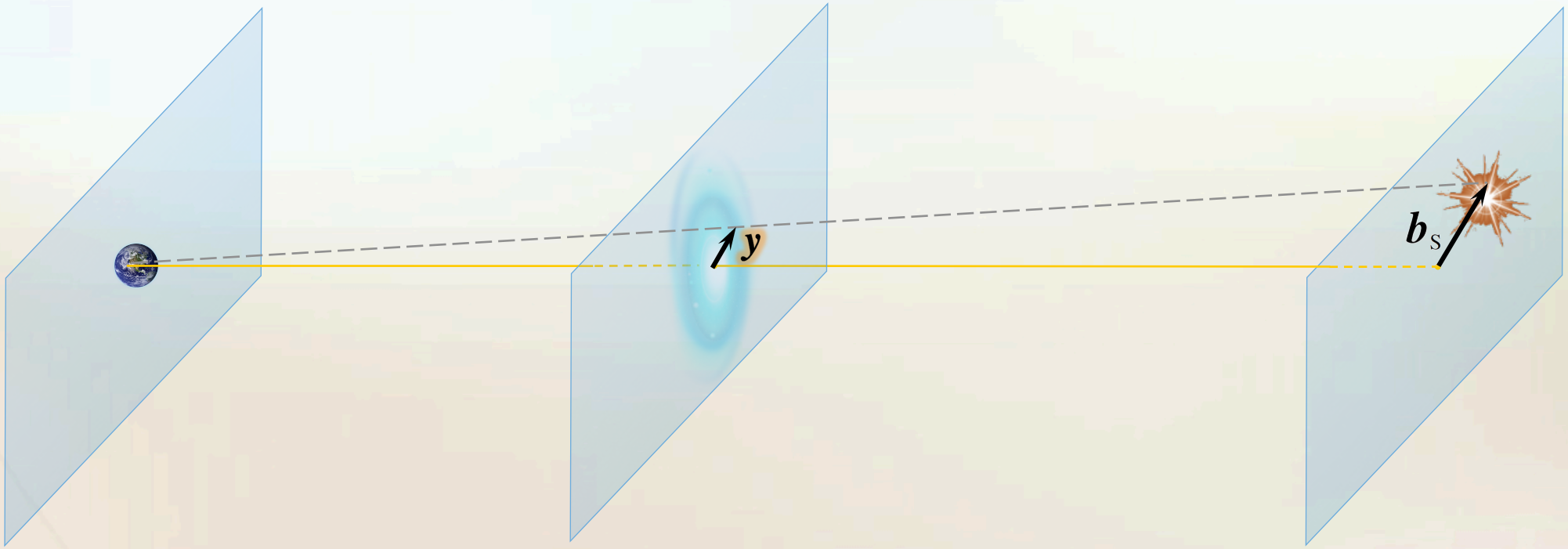

1 The adimensional lens equation

$$\boldsymbol{y} = \boldsymbol{x} + \hat{\boldsymbol{\alpha}}(\boldsymbol{x}) \longrightarrow = ?$$

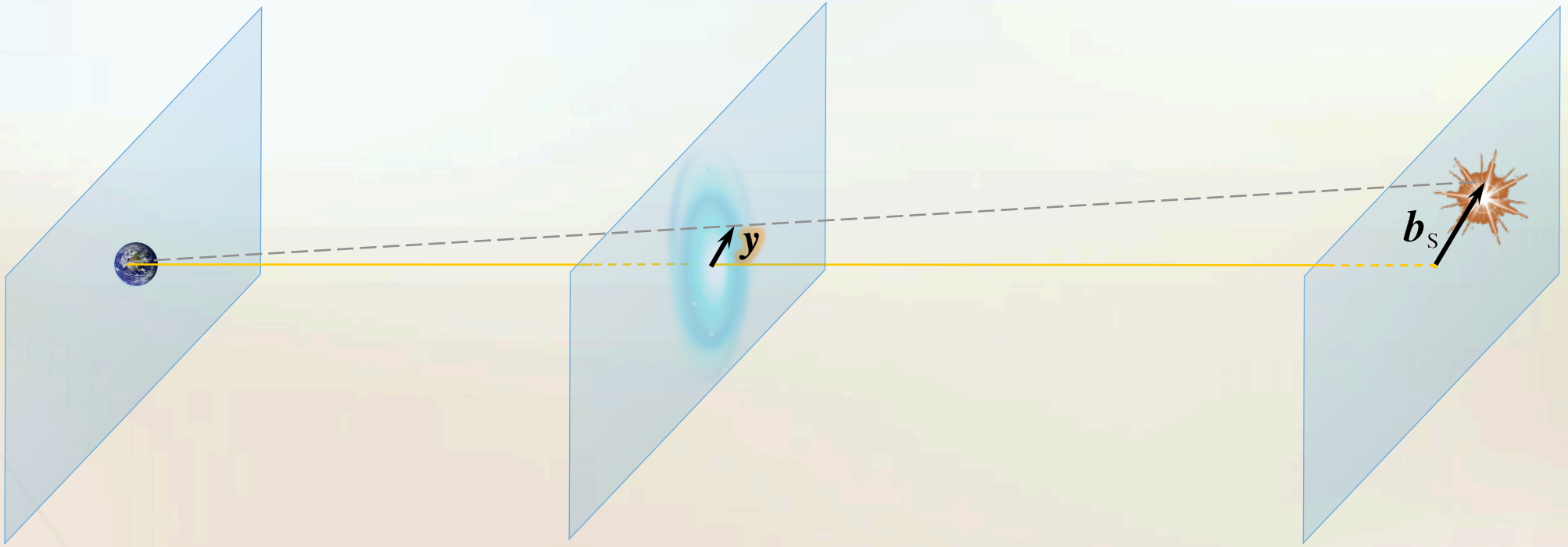

1 Analytical solutions ? $y = x + \hat{\alpha}(x$

- The point-like deflector $\hat{\alpha}(x) = -\frac{x}{|x|^2}$
- The singular isothermal sphere (SIS)

$$\left.\begin{aligned} \kappa(x) &= \delta(x) \\ \hat{\alpha}(x) &= -\frac{x}{|x|^2} \end{aligned}\right\} \quad |x| = \frac{1}{2}\left(|y| \pm \sqrt{|y|^2+4}\right)$$

1 Analytical solutions ? $\boldsymbol{y} = \boldsymbol{x} + \hat{\boldsymbol{\alpha}}(\boldsymbol{x})$

- The point-like deflector $\hat{\alpha}(x) = -\frac{x}{|x|^2}$
- The singular isothermal sphere (SIS) $\hat{\alpha}(x) = -\frac{x}{|x|}$
- The infinite sheet of constant surface mass density

$$\kappa(\boldsymbol{x}) = \frac{1}{2|\boldsymbol{x}|}$$

$$\hat{\boldsymbol{\alpha}}(\boldsymbol{x}) = -\frac{\boldsymbol{x}}{|\boldsymbol{x}|}$$

$$|\boldsymbol{x}| = |\boldsymbol{y}| \pm 1 \quad \text{if} \quad |\boldsymbol{y}| < 1$$

$$|\boldsymbol{x}| = |\boldsymbol{y}| + 1 \quad \text{otherwise}$$

1 Analytical solutions ? $\boldsymbol{y} = \boldsymbol{x} + \hat{\boldsymbol{\alpha}}(\boldsymbol{x})$

- The point-like deflector $\hat{\alpha}(x) = -\frac{x}{|x|^2}$
- The singular isothermal sphere (SIS) $\hat{\alpha}(x) = -\frac{x}{|x|}$
- The infinite sheet of constant surface mass density $\hat{\alpha}(x) = -\kappa\, x$

$$\left.\begin{aligned} \kappa(\boldsymbol{x}) &= \kappa \\ \hat{\boldsymbol{\alpha}}(\boldsymbol{x}) &= -\kappa\, \boldsymbol{x} \end{aligned}\right\} \quad |\boldsymbol{x}| = \frac{|\boldsymbol{y}|}{|1-\kappa|}$$

1 Analytical solutions ? $\boldsymbol{y} = \boldsymbol{x} + \hat{\boldsymbol{\alpha}}(\boldsymbol{x})$

- The point-like deflector $\hat{\boldsymbol{\alpha}}(\boldsymbol{x}) = -\frac{\boldsymbol{x}}{|\boldsymbol{x}|^2}$ $\varepsilon = 0$
- The singular isothermal sphere (SIS) $\hat{\boldsymbol{\alpha}}(\boldsymbol{x}) = -\frac{\boldsymbol{x}}{|\boldsymbol{x}|}$ $\varepsilon = 1$
- The infinite sheet of constant surface mass density $\hat{\boldsymbol{\alpha}}(\boldsymbol{x}) = -\kappa\, \boldsymbol{x}$ ε

$$\hat{\boldsymbol{\alpha}}(\boldsymbol{x}) = -|\boldsymbol{x}|^{\varepsilon-2}\, \boldsymbol{x}$$

1 Analytical solutions ? $\boldsymbol{y} = \boldsymbol{x} + \hat{\boldsymbol{\alpha}}(\boldsymbol{x})$

- The point-like deflector $\hat{\boldsymbol{\alpha}}(\boldsymbol{x}) = -\frac{\boldsymbol{x}}{|\boldsymbol{x}|^2}$ $\varepsilon = 0$
- The singular isothermal sphere (SIS) $\hat{\boldsymbol{\alpha}}(\boldsymbol{x}) = -\frac{\boldsymbol{x}}{|\boldsymbol{x}|}$ $\varepsilon = 1$
- The infinite sheet of constant surface mass density $\hat{\boldsymbol{\alpha}}(\boldsymbol{x}) = -\kappa\, \boldsymbol{x}$ ε

$$\hat{\boldsymbol{\alpha}}(\boldsymbol{x}) = -|\boldsymbol{x}|^{\varepsilon-2}\, \boldsymbol{x}$$

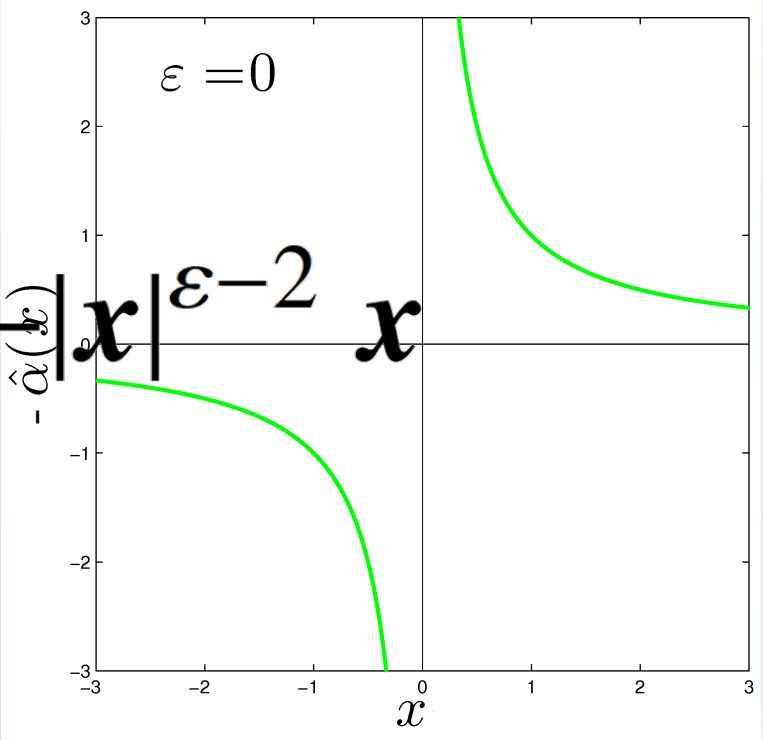

The GL experiment

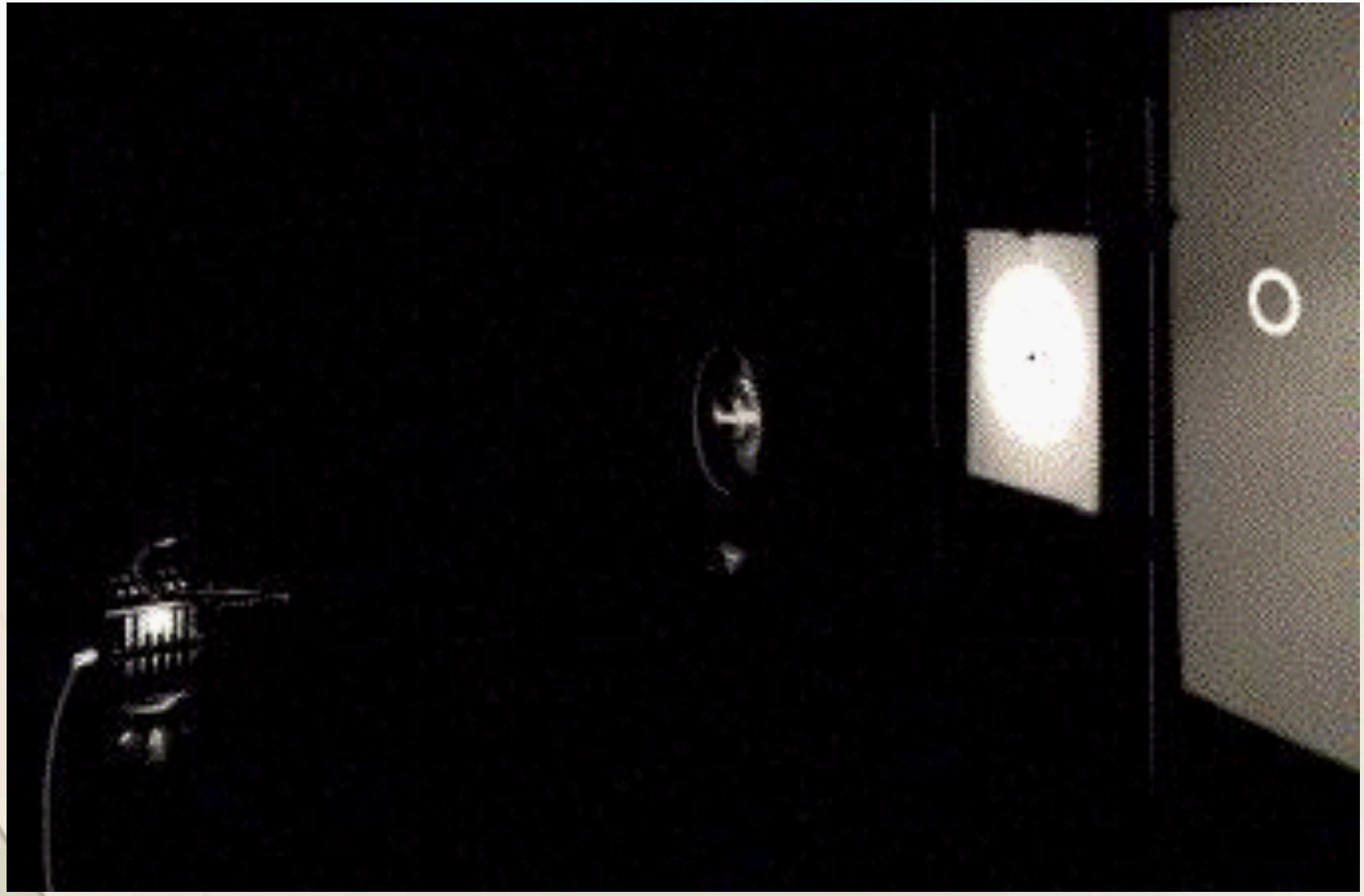

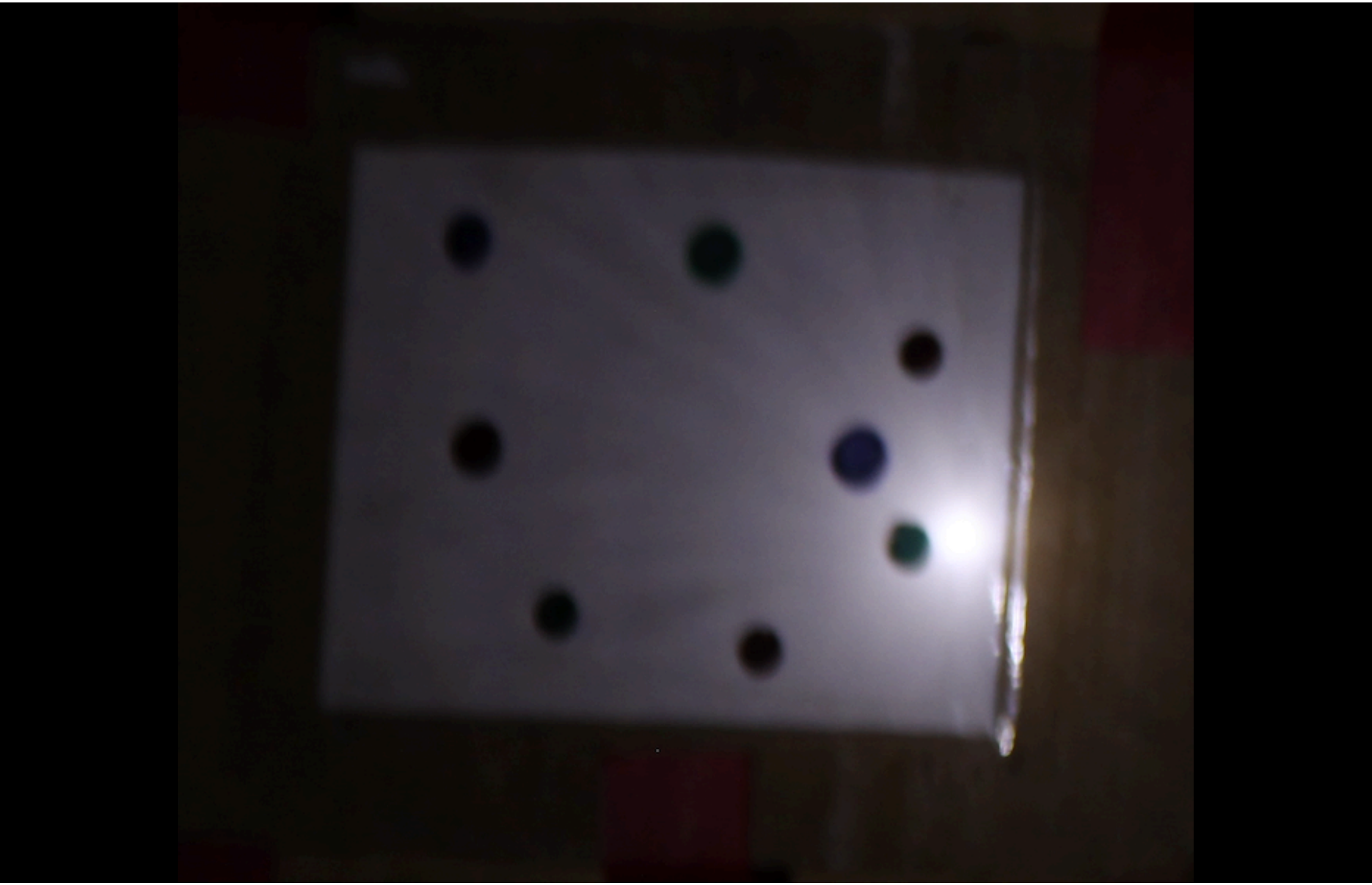

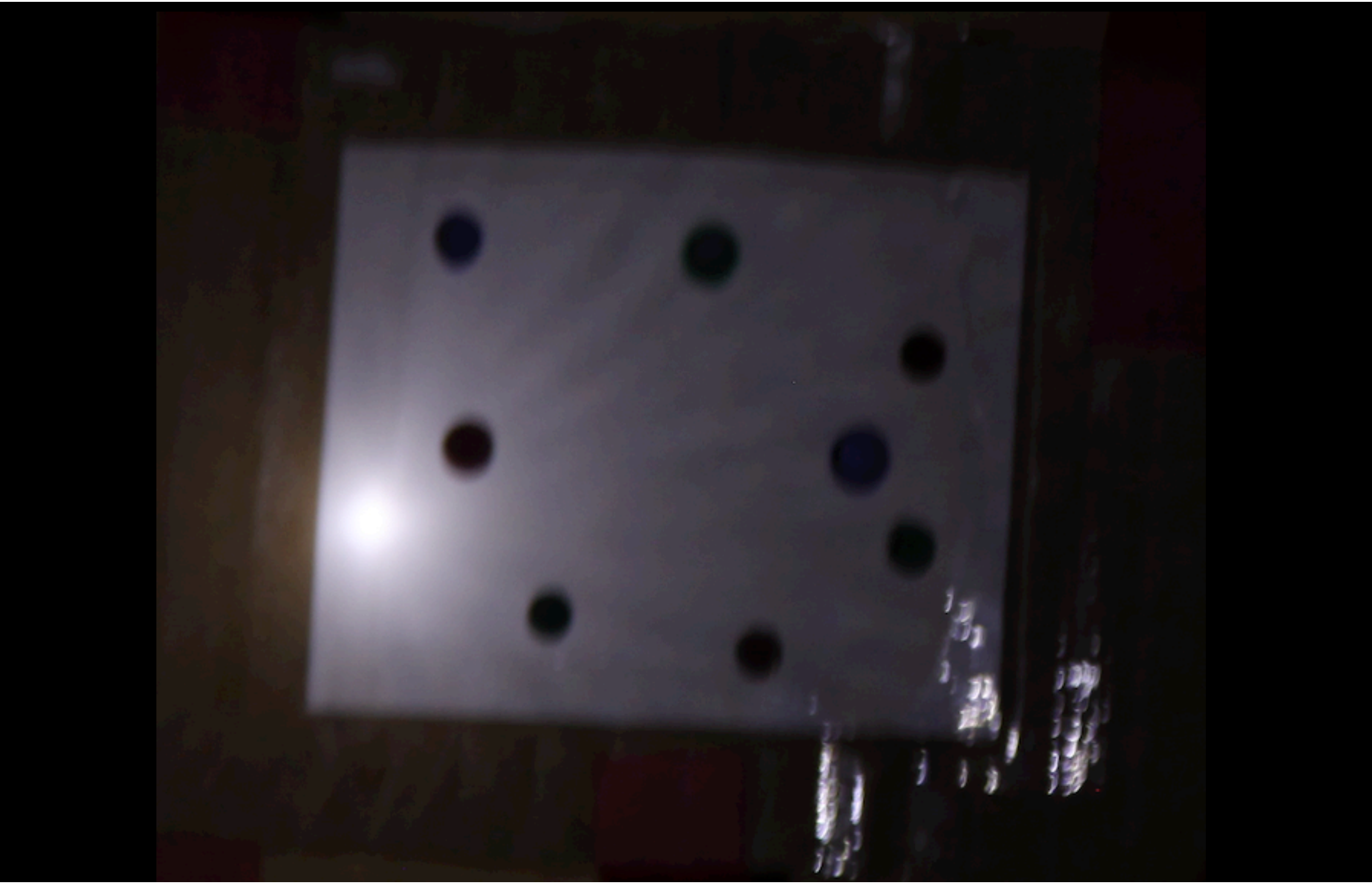

$\varepsilon = 0.9$

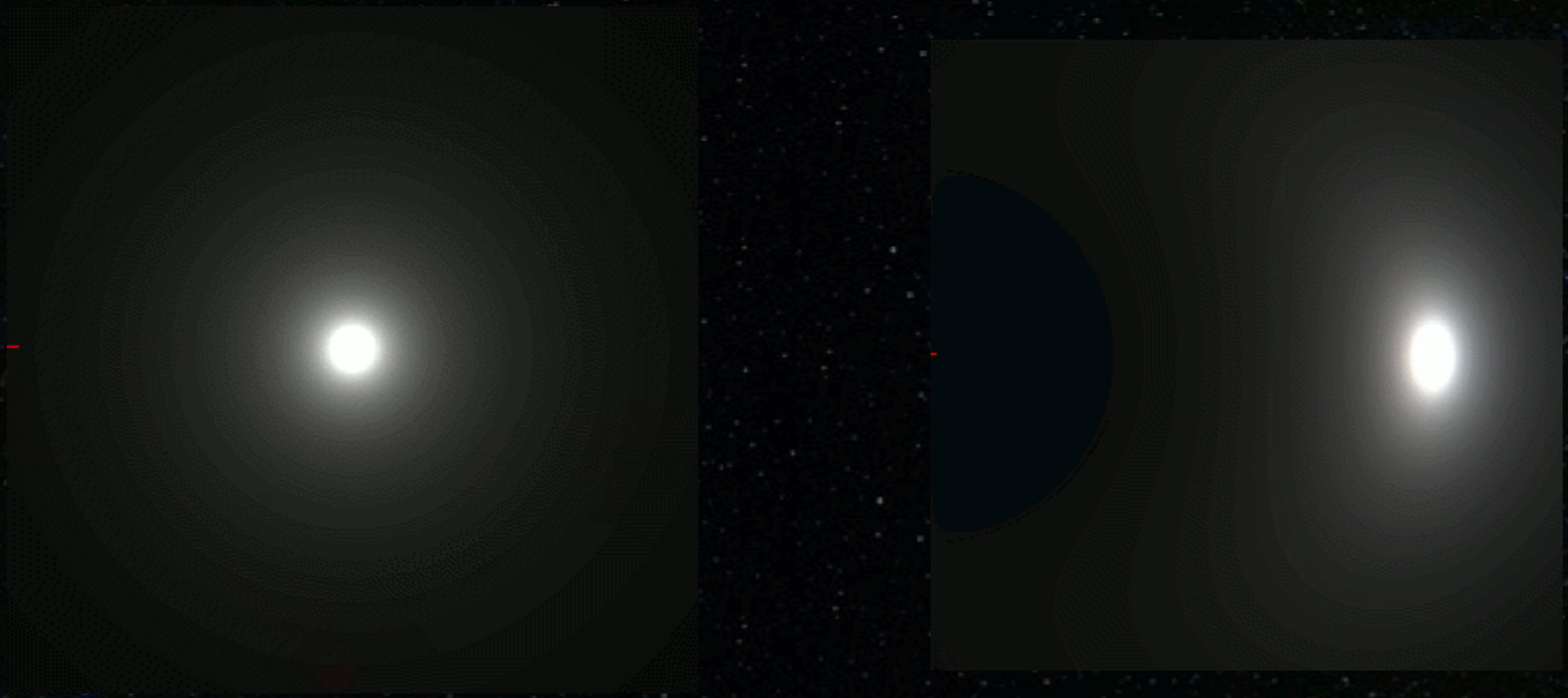

Amplification ratio $\mu^{(1)}/\mu^{(2)}$

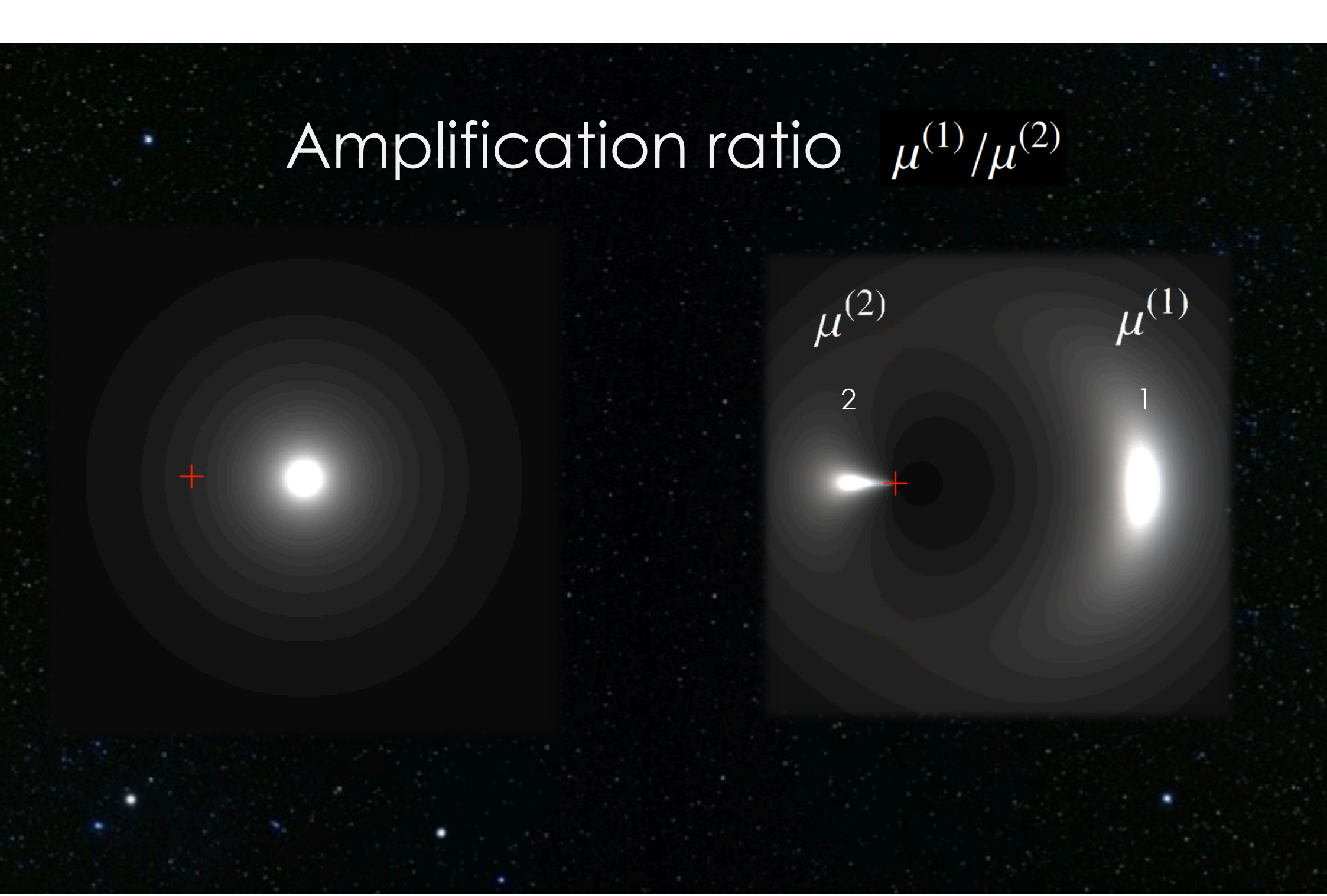

Einstein ring angular radius $\theta_{\mathrm{E}} D_{\mathrm{OD}} = b$

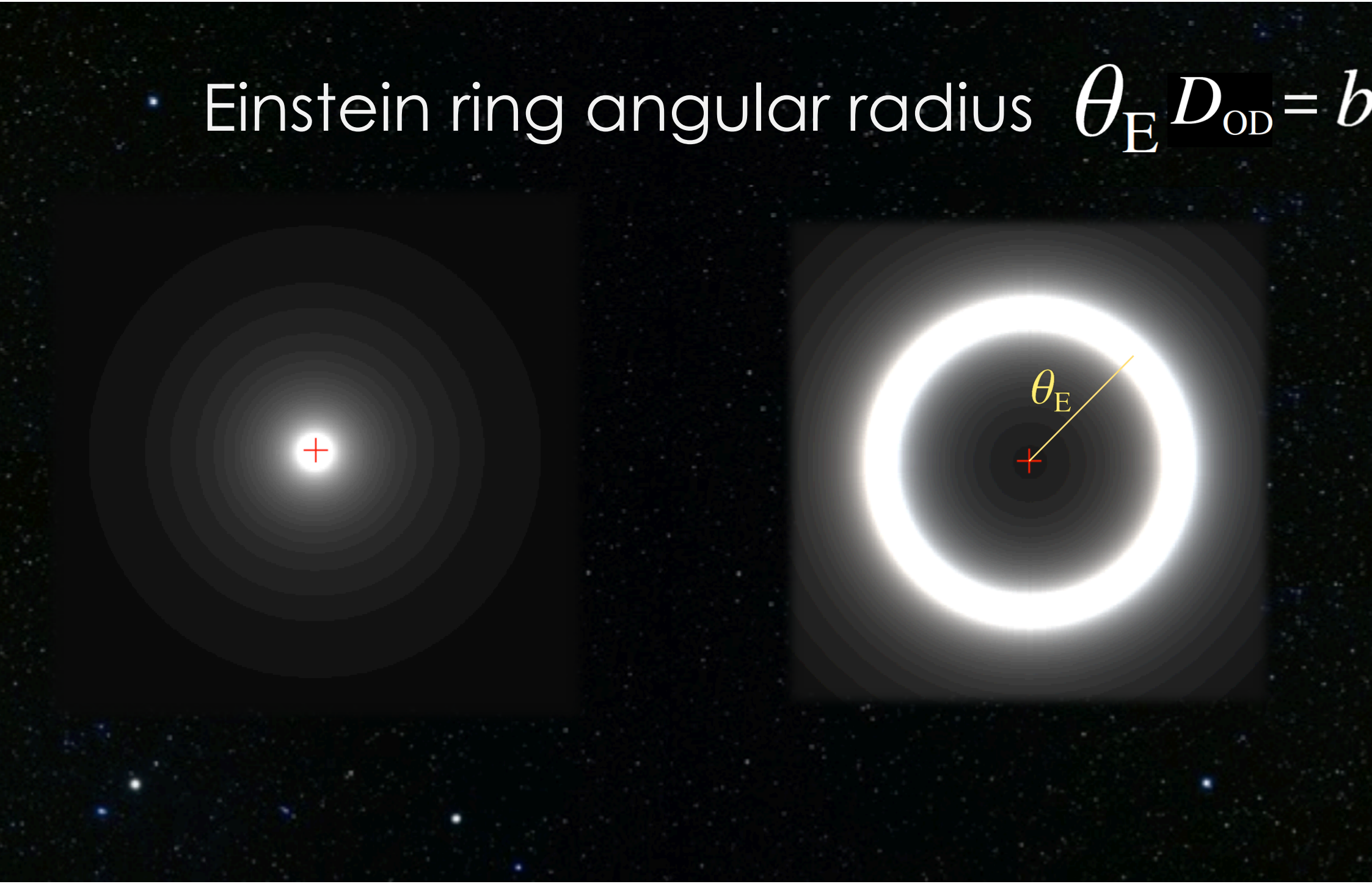

The adimensional lens equation

$$\boldsymbol{y} = \boldsymbol{x} + \hat{\boldsymbol{\alpha}}(\boldsymbol{x})$$

$$\frac{D_{OD}}{D_{OS}}\frac{\boldsymbol{b}_S}{\boldsymbol{b}_0} = \frac{\boldsymbol{b}}{\boldsymbol{b}_0} + \frac{D_{OD}D_{DS}}{\boldsymbol{b}_0 D_{OS}}\boldsymbol{\alpha}(\boldsymbol{b})$$

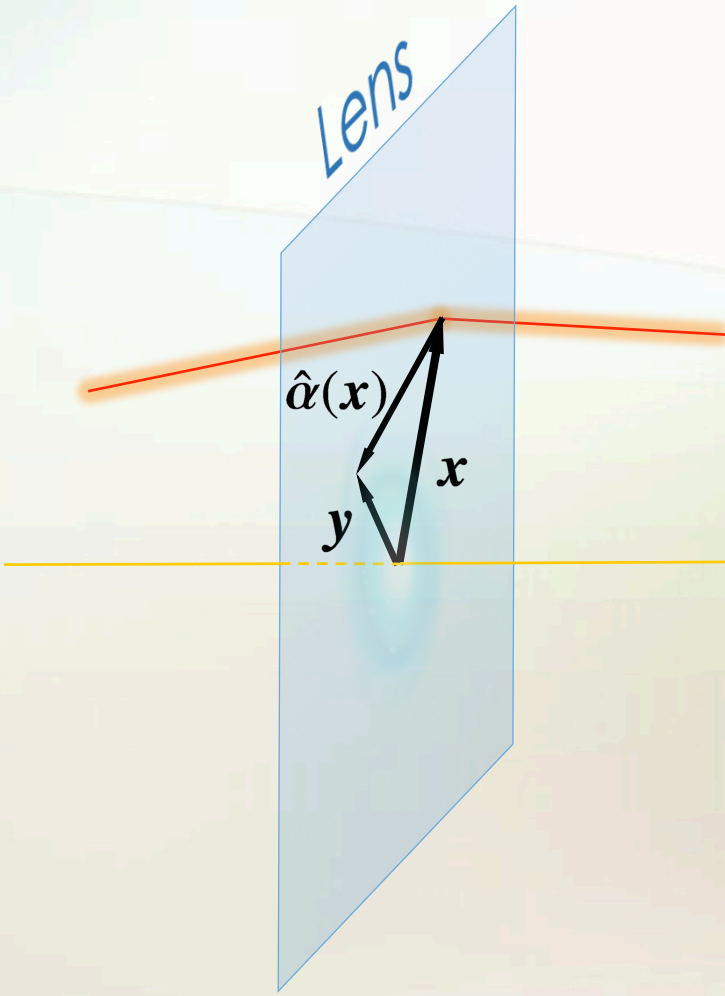

- Einstein ring angular radius $\theta_{\mathrm{E}} D_{\mathrm{OD}} = b$

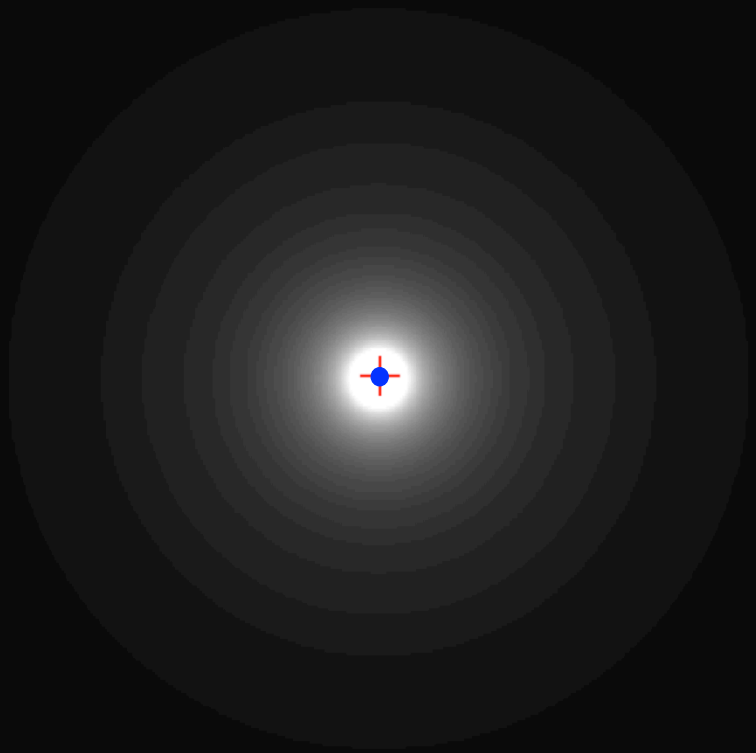

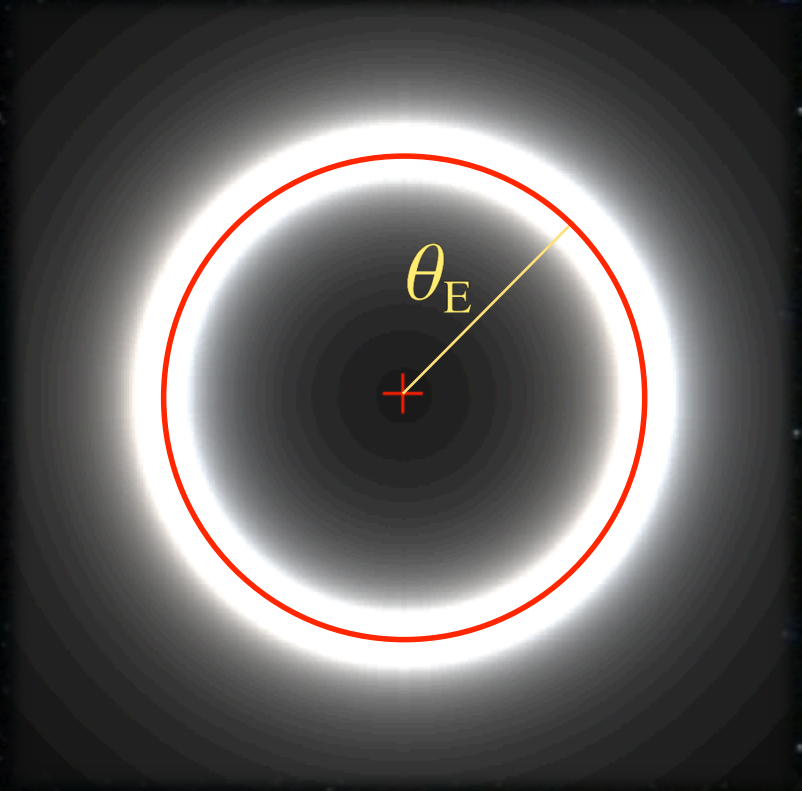

caustic line(s)

critical line(s)

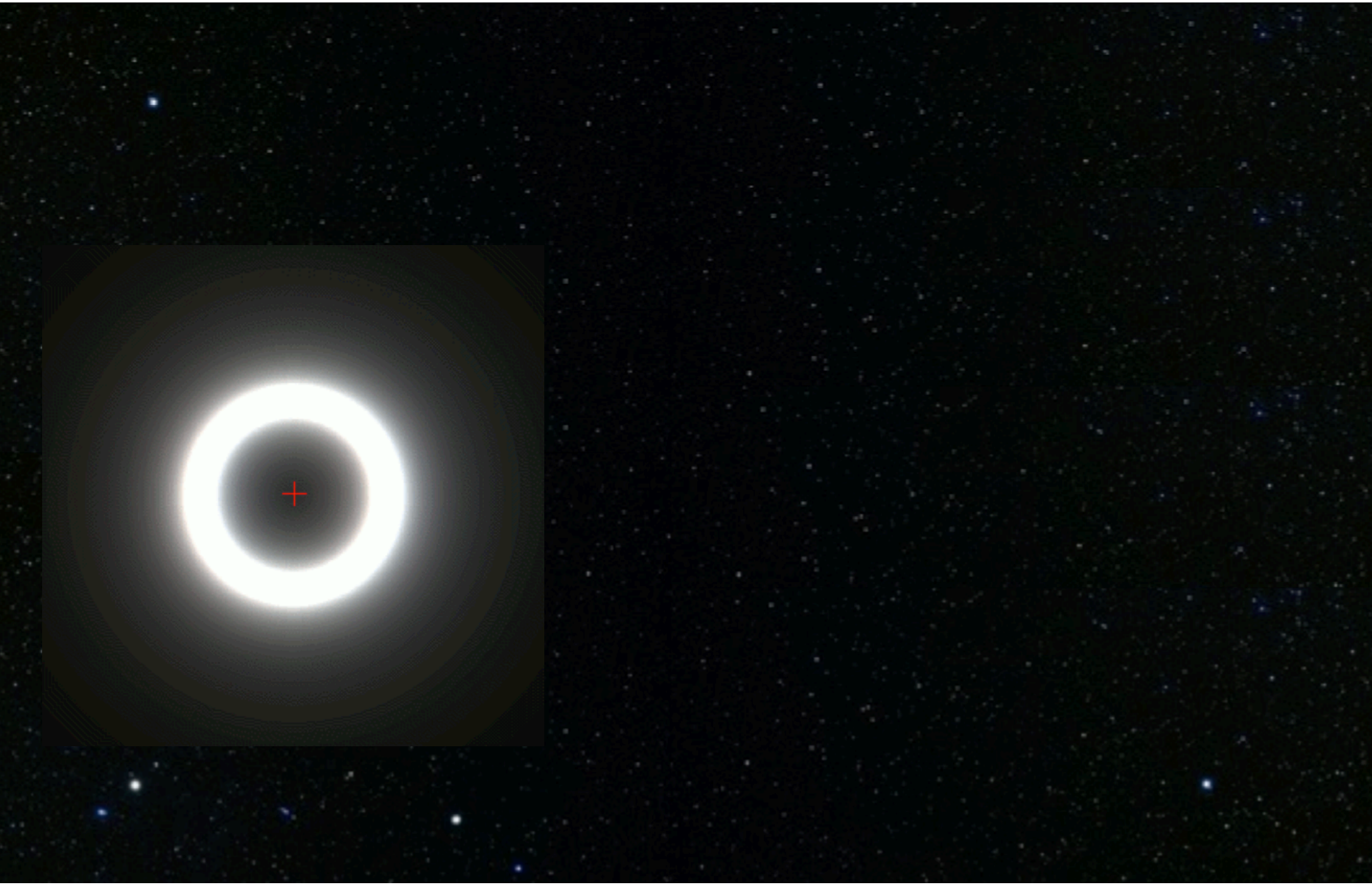

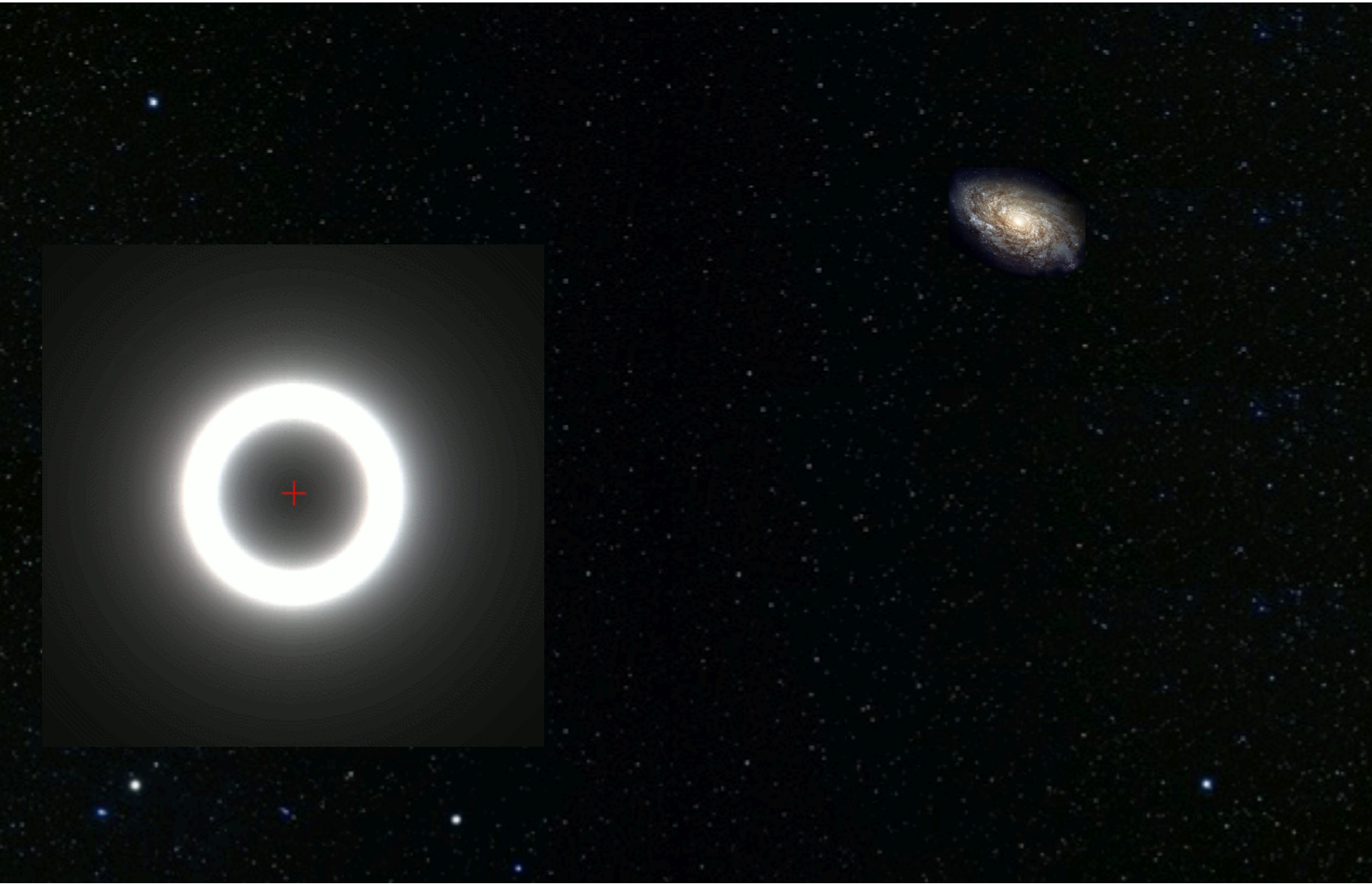

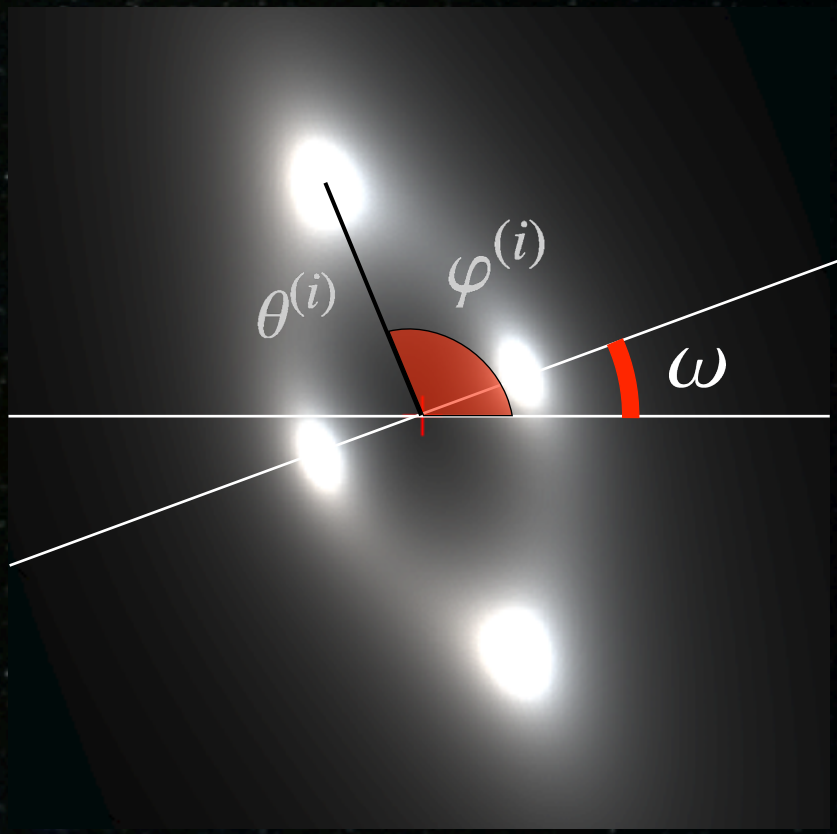

shear strength γ

shear orientation ω

$\varepsilon = 0.9$ $\gamma = 0.1$ $\omega = -\pi/8$

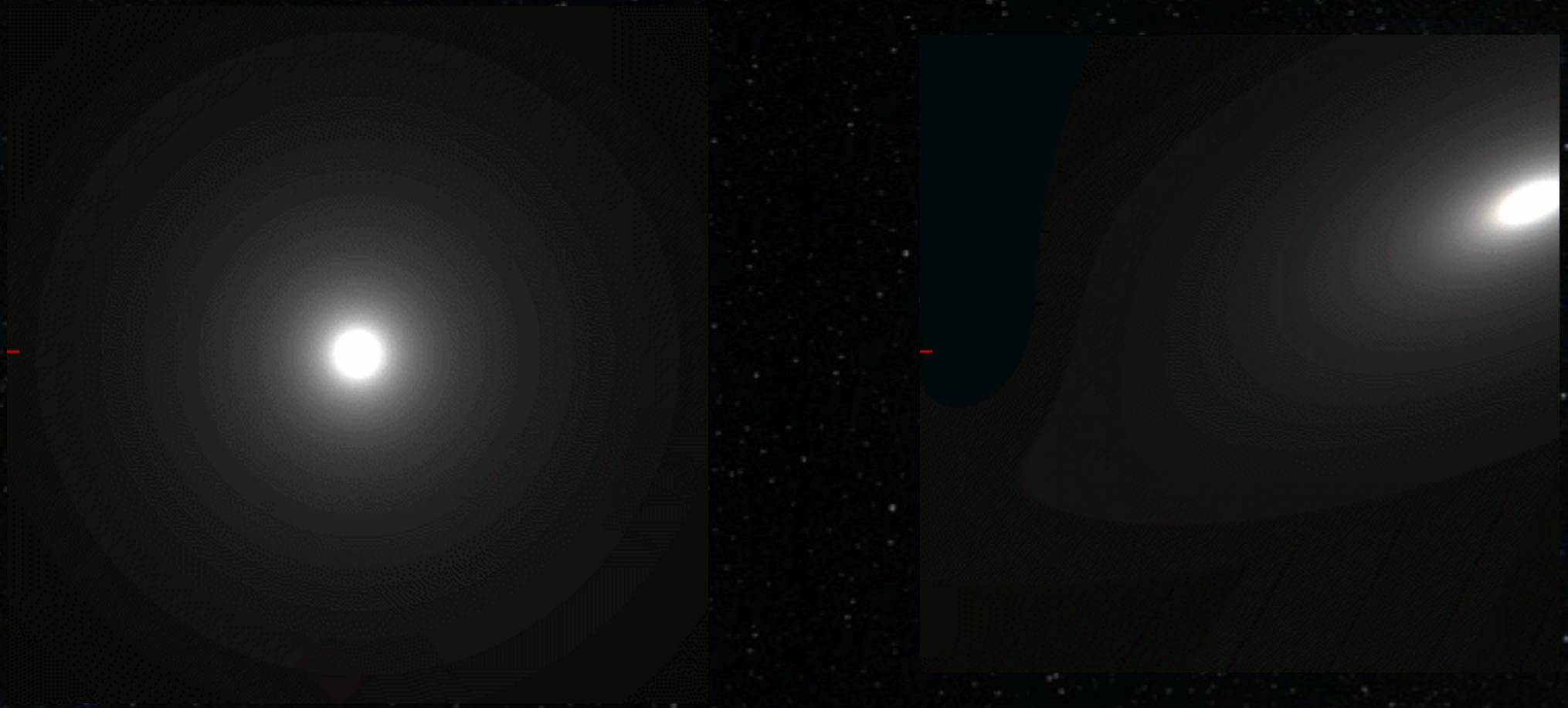

1 The so-called ε-γ models

$$\hat{\boldsymbol{\alpha}}(\boldsymbol{x}) = -|\boldsymbol{x}|^{\varepsilon-2}\,\boldsymbol{x} + \gamma\,\mathcal{S}^{*}\mathcal{F}$$

6 model parameters

θ_S, θ, θ_E, ε, γ and ω

8 constraints

$\theta^{(i)}$ and $\varphi^{(i)}$

$$p_k = F_k\left(\theta^{(i)}, \varphi^{(i)}\right)$$

$$\omega = \frac{1}{4}\left(\varphi^{(0)} + \varphi^{(1)} + \varphi^{(2)} + \varphi^{(3)} - 3\right.$$

$$H_0 = F\left(z, \Delta t, \Omega_\Lambda, \theta^{(i)}, \varphi^{(i)}\right)$$

Wertz, Pelgrims and Surdej (2

The singular isothermal ellipsoid (SIE) models

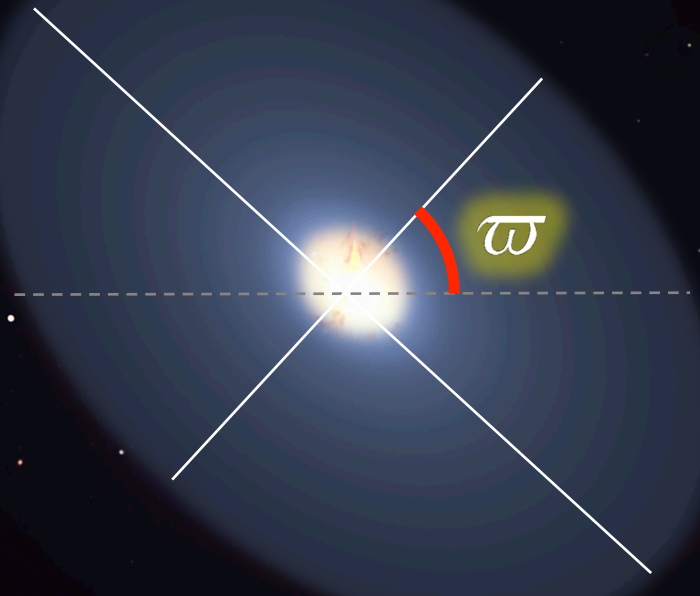

$$\kappa(x_1, x_2) = \frac{\sqrt{f}}{2\sqrt{x_1^2 + f}}$$

2 The singular isothermal ellipsoid (SIE) models

5 model parameters

$\theta_S, \theta, \theta_E, f$ and ϖ

8 constraints

$\theta^{(i)}$ and $\varphi^{(i)}$

$$p_k = F_k\left(\theta^{(i)}, \varphi^{(i)}\right)$$

$$\theta_s = \frac{1}{2}\sqrt{(\theta^{(0)} - \theta^{(2)})^2 + (\theta^{(1)} - \theta^{(3)}}$$

$$H_0 = F\left(z, \Delta t, \Omega_\Lambda, \theta^{(i)}, \varphi^{(i)}\right)$$

Witt et al. (2000)

3 The non-singular isothermal ellipsoid (NSIE)

$$\kappa(\boldsymbol{x}) = \kappa(\rho) \quad \text{where} \quad \rho = \sqrt{x_1^2 + f^2 x_2^2}$$

$$\kappa(\rho) = \frac{\sqrt{f}}{2\sqrt{\rho^2 + \rho_c^2}}$$

Fourier

Wertz & Surdej (2014)

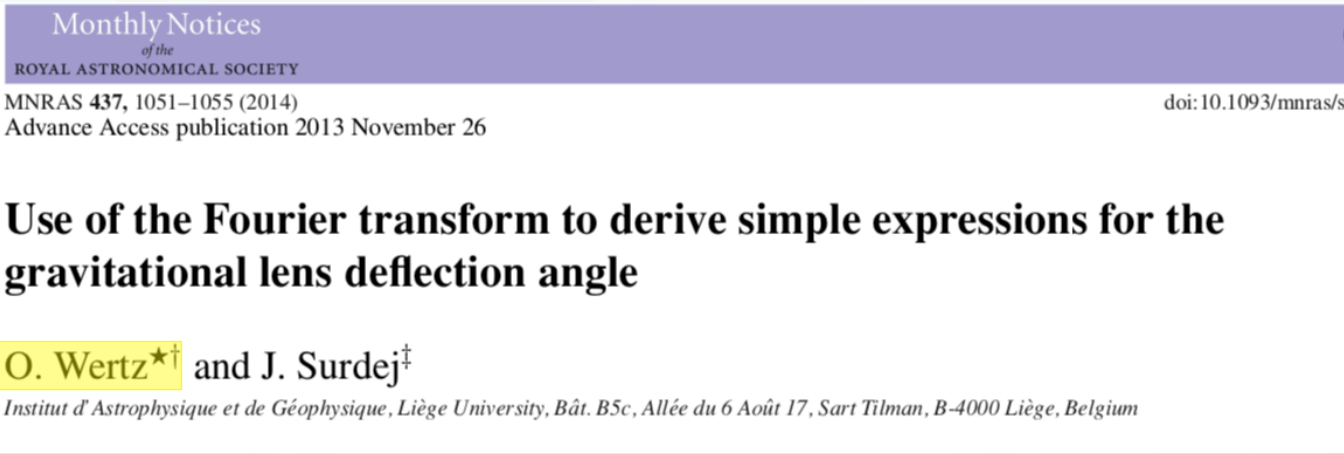

Monthly Notices of the ROYAL ASTRONOMICAL SOCIETY

MNRAS **437,** 1051–1055 (2014) doi:10.1093/mnras/s
Advance Access publication 2013 November 26

Use of the Fourier transform to derive simple expressions for the gravitational lens deflection angle

O. Wertz★† and J. Surdej‡
Institut d'Astrophysique et de Géophysique, Liège University, Bât. B5c, Allée du 6 Août 17, Sart Tilman, B-4000 Liège, Belgium

$\hat{\boldsymbol{\alpha}}(\boldsymbol{x})$

$\hat{\psi}(\boldsymbol{x})$

caustic and critical curves

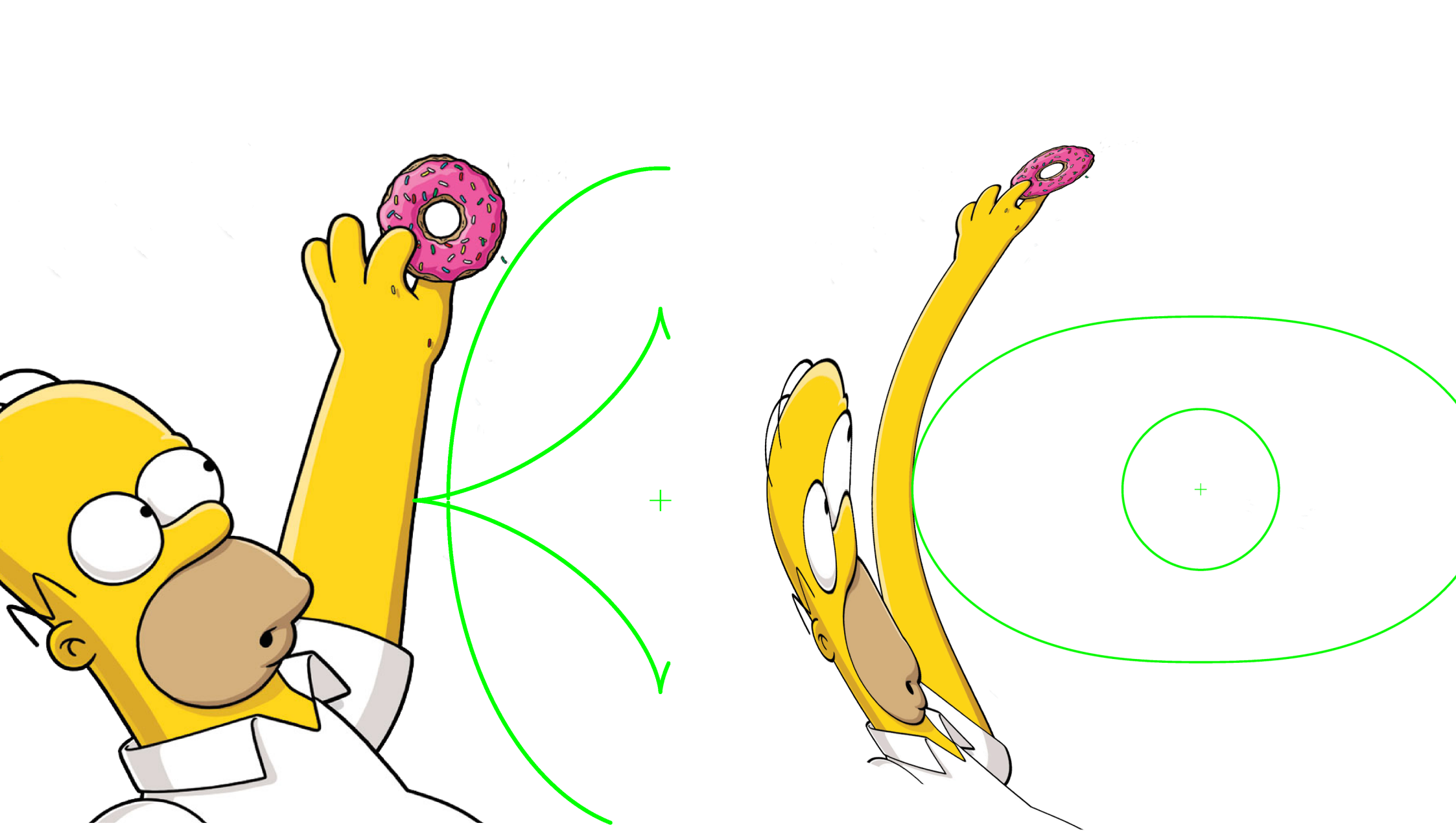

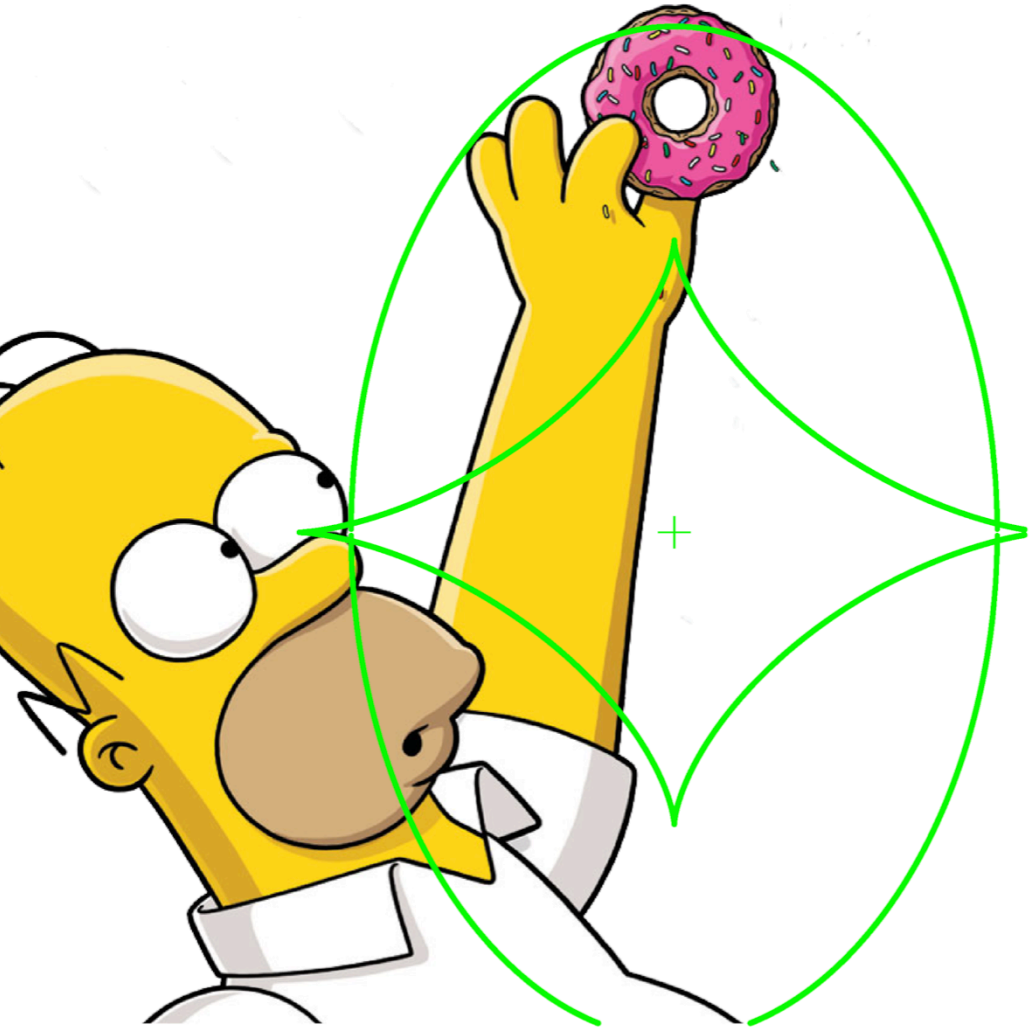

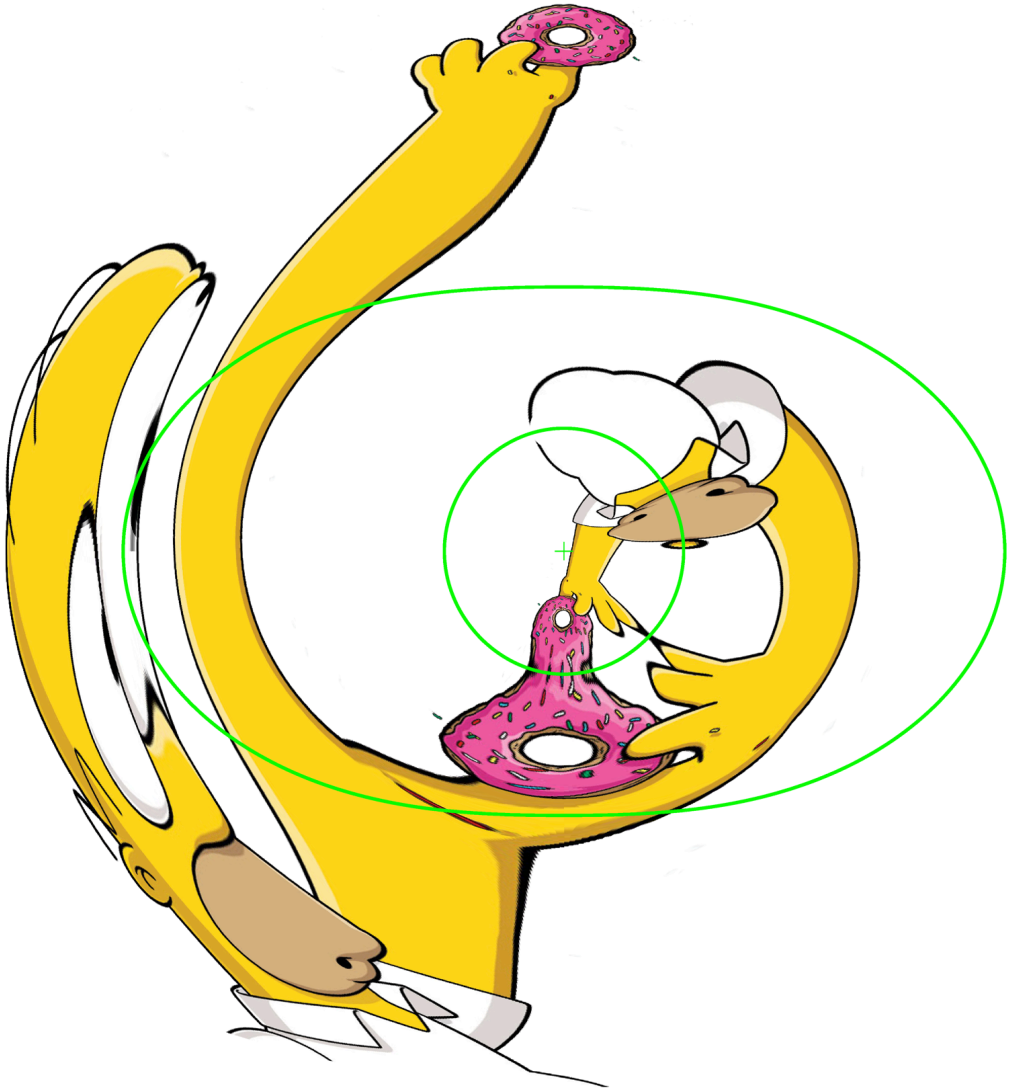

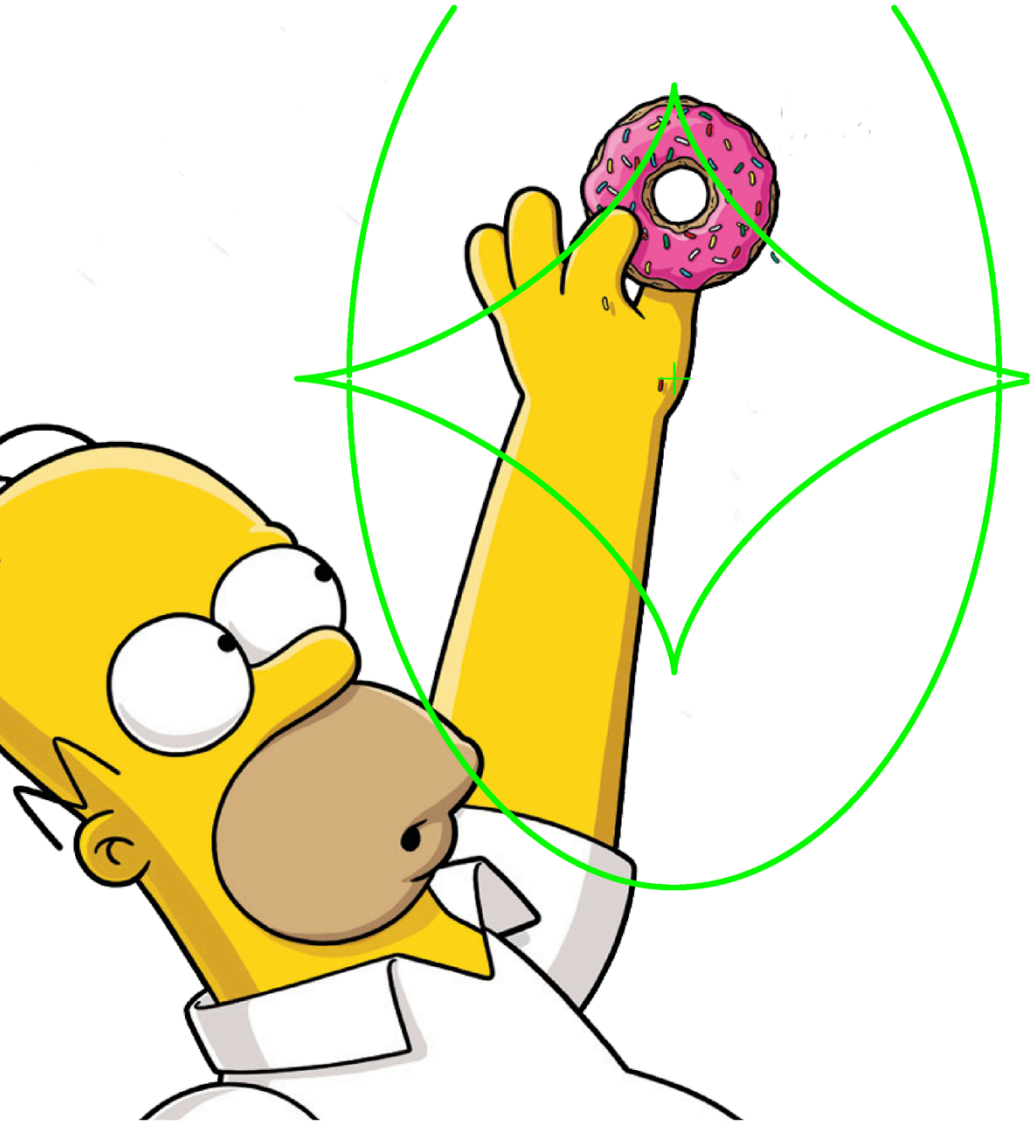

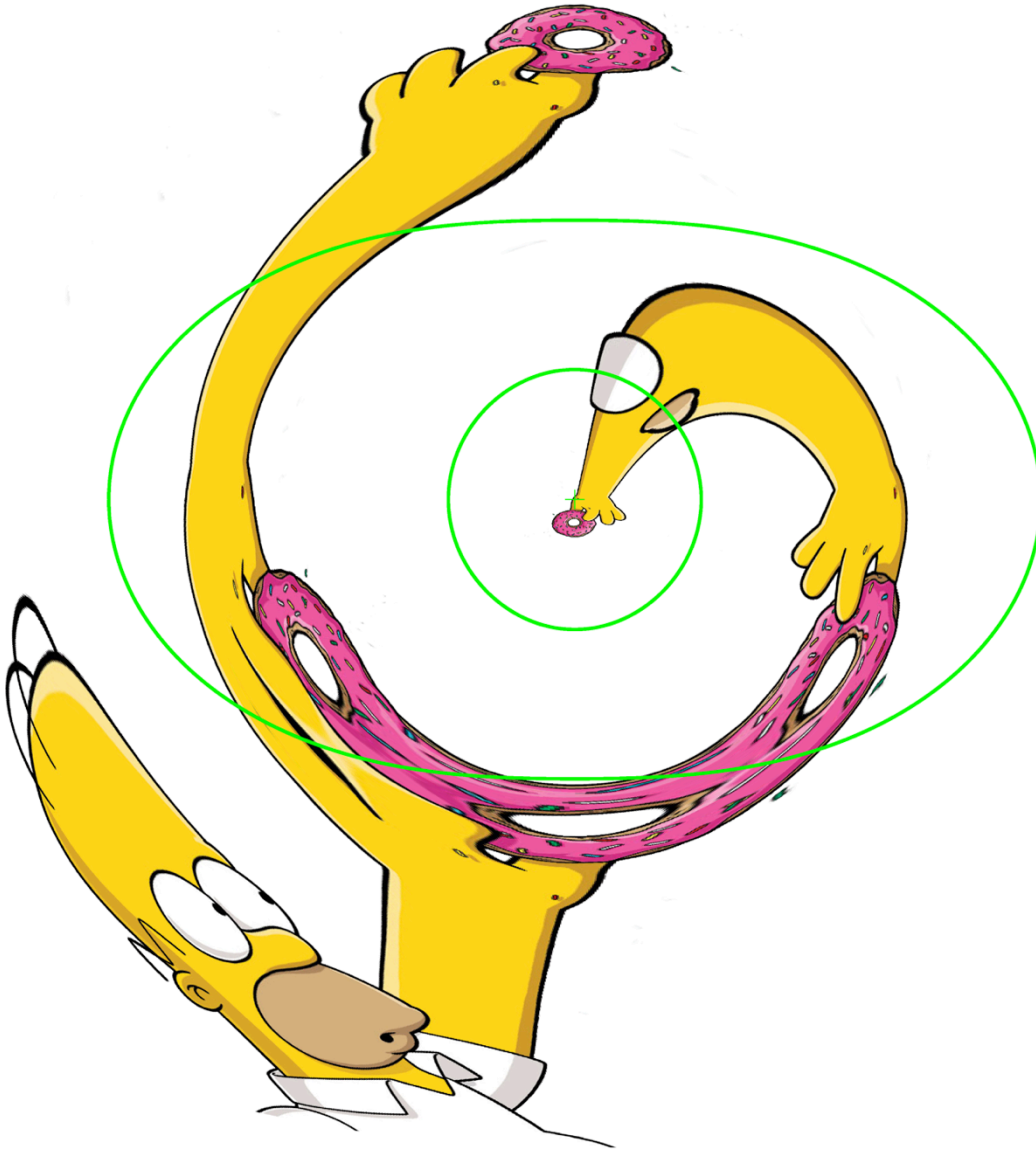

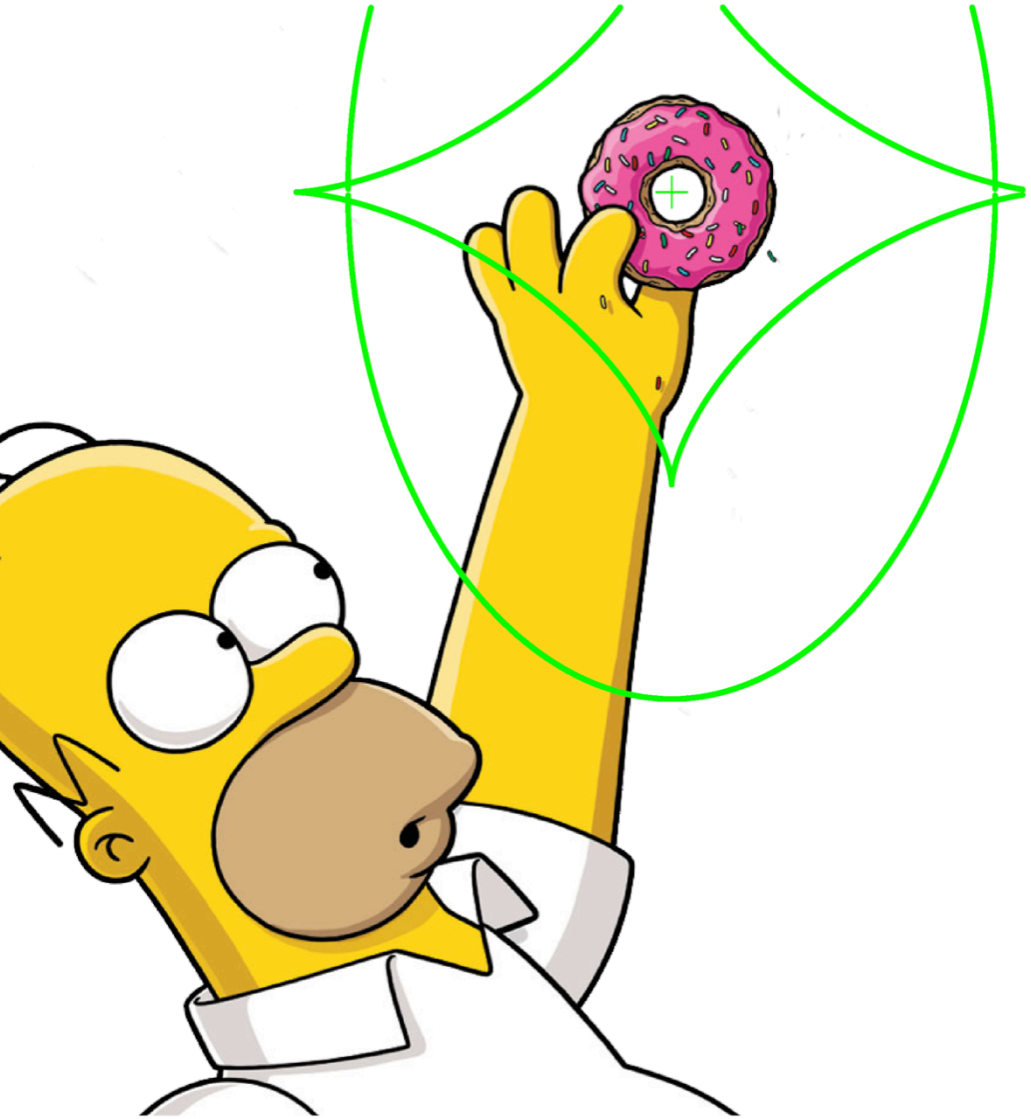

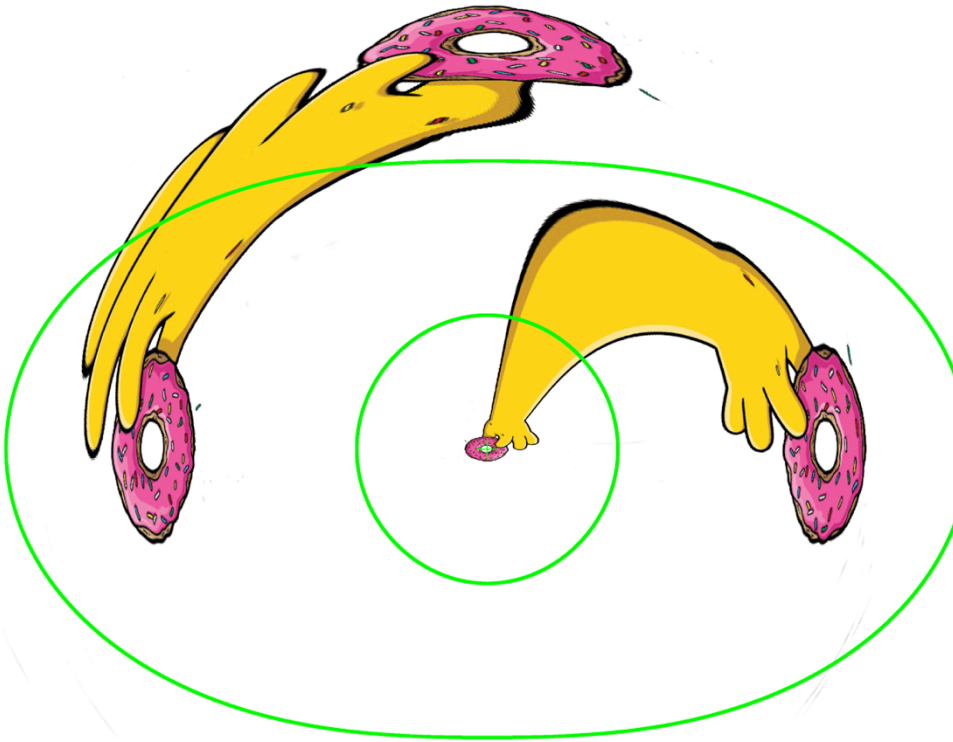

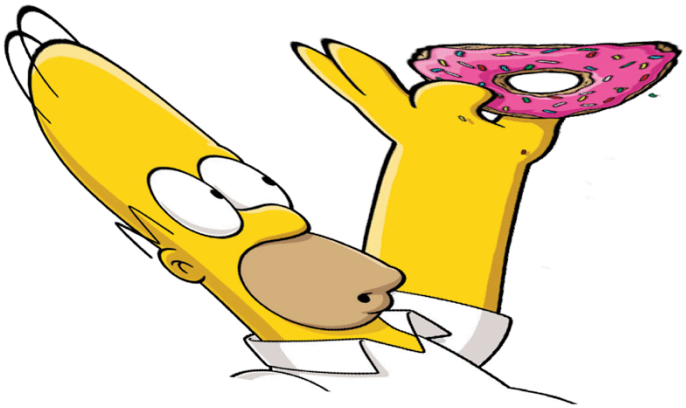

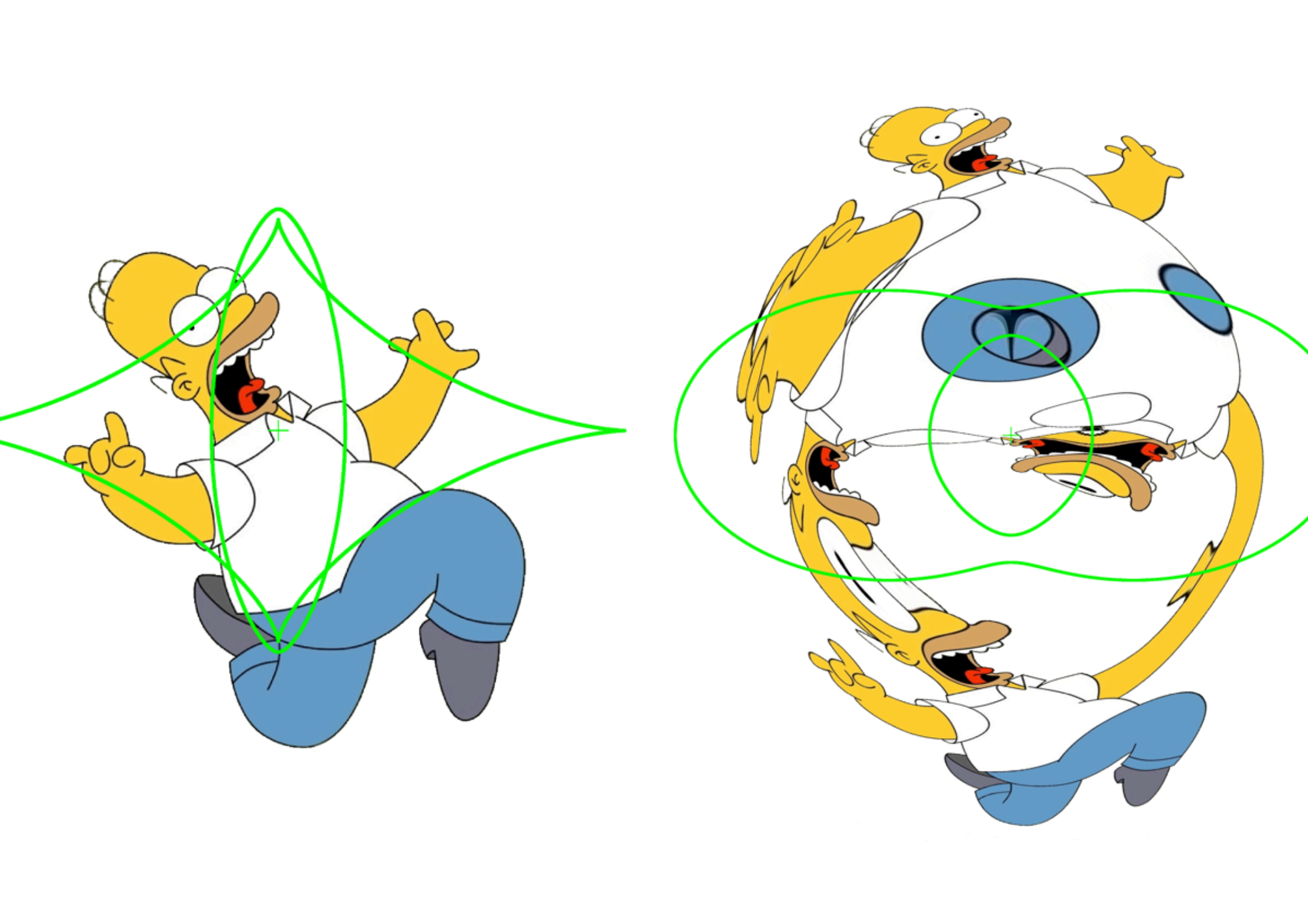

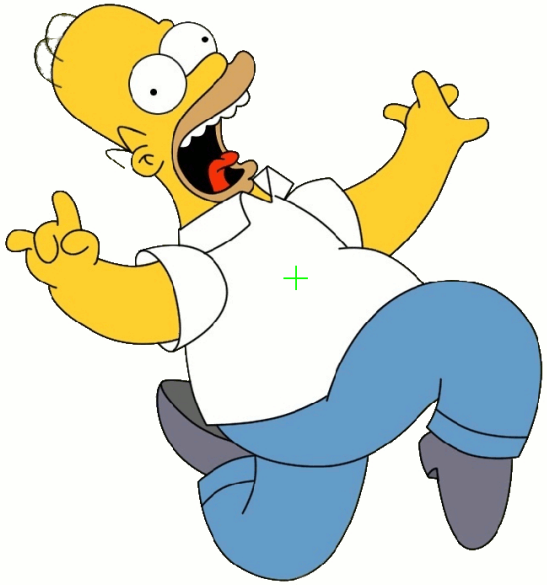

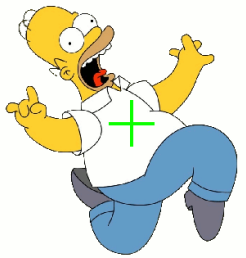

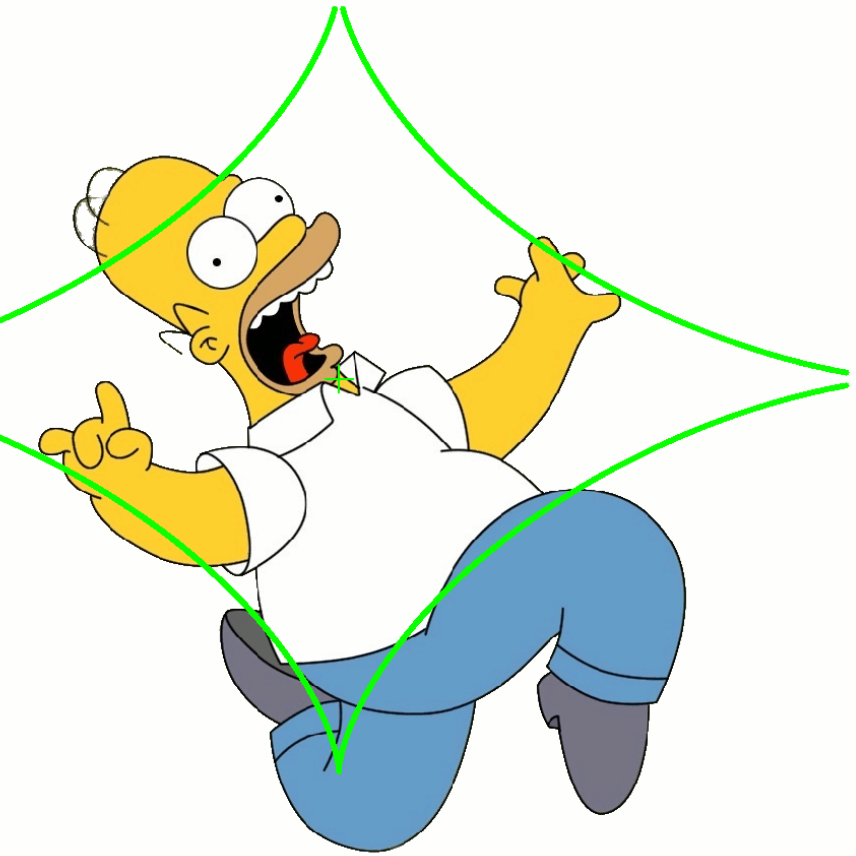

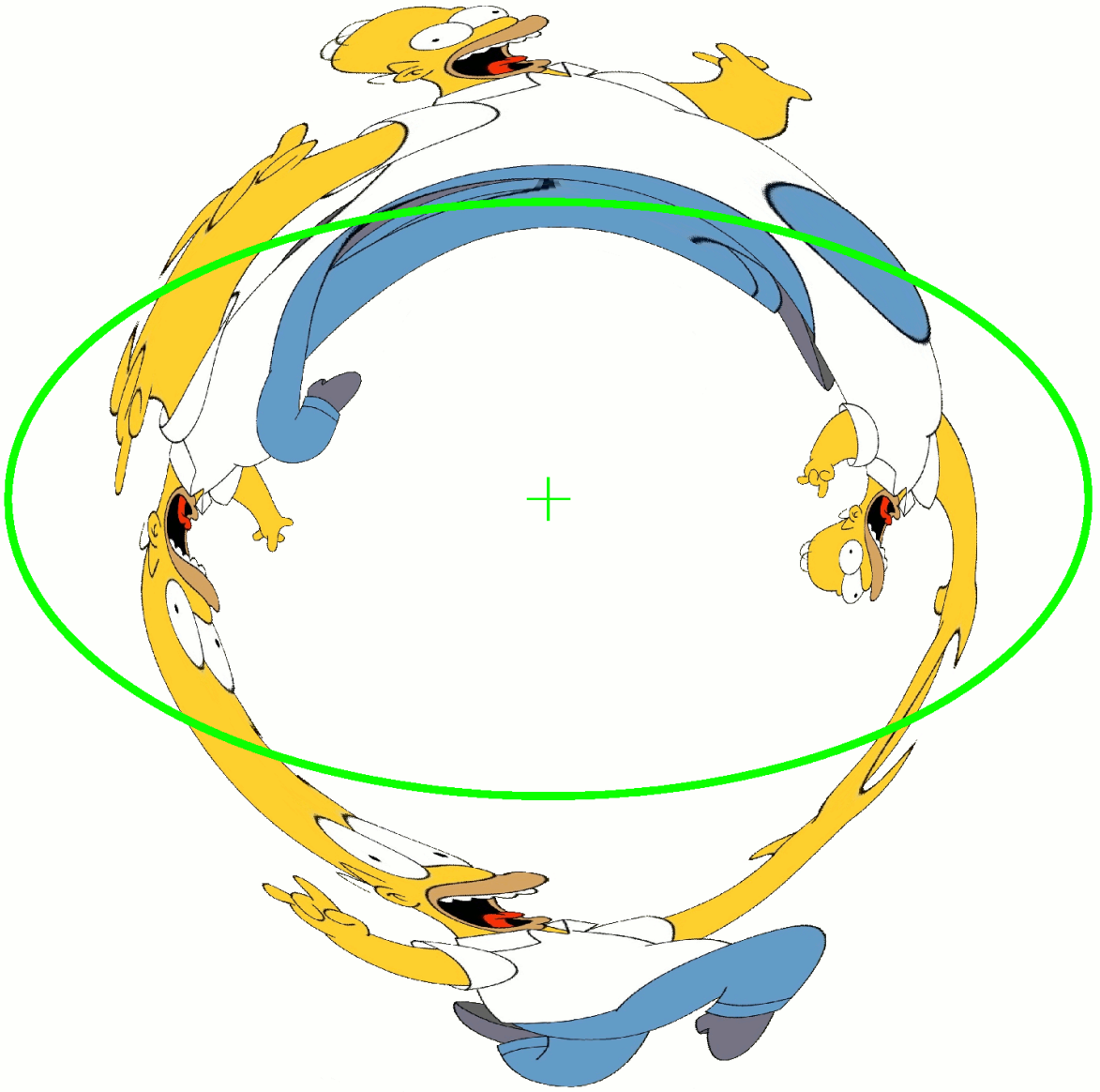

590, A42 (2016)
10.1051/0004-6361/201425411
© 2016

Astronomy & Astrophysics

Multiply imaged quasi-stellar objects in the *Gaia* survey

F. Finet[1,2] and J. Surdej[1]

[1] Extragalactic Astrophysics and Space Observations (AEOS), Institut d'Astrophysique et de Géophysique, Liège University, Allée du 6 Août, 17 (Sart Tilman, Bât. B5c), 4000 Liège, Belgium
[2] National Astronomical Observatory of Japan (NAOJ), 650 N. A'ohoku Place, Hilo, 96720 HI, USA
e-mail: finet@naoj.org

Lensing probability

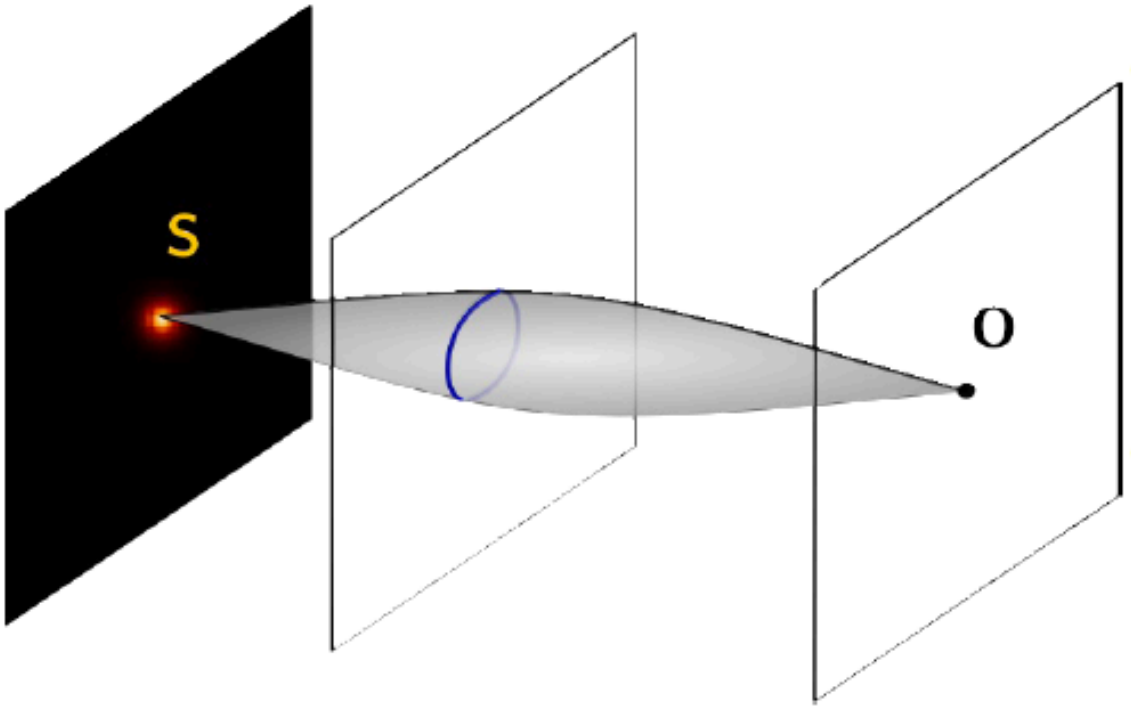

- Lensing volume: envelope of the lensing cross sections
- Integrate deflector density in the volume
- Different volumes for different cross sections considered

SIE Cross section:

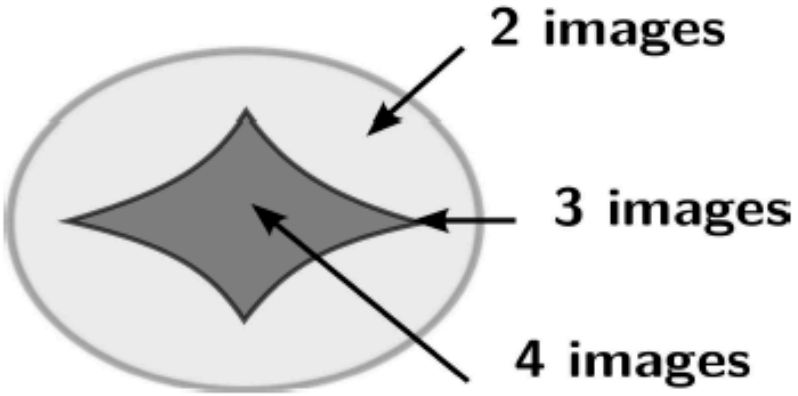

KS J11331-1231 (Sluse et al. 2003, 005, Claeskens et al. 2006) : z_s=0.658, =0.295

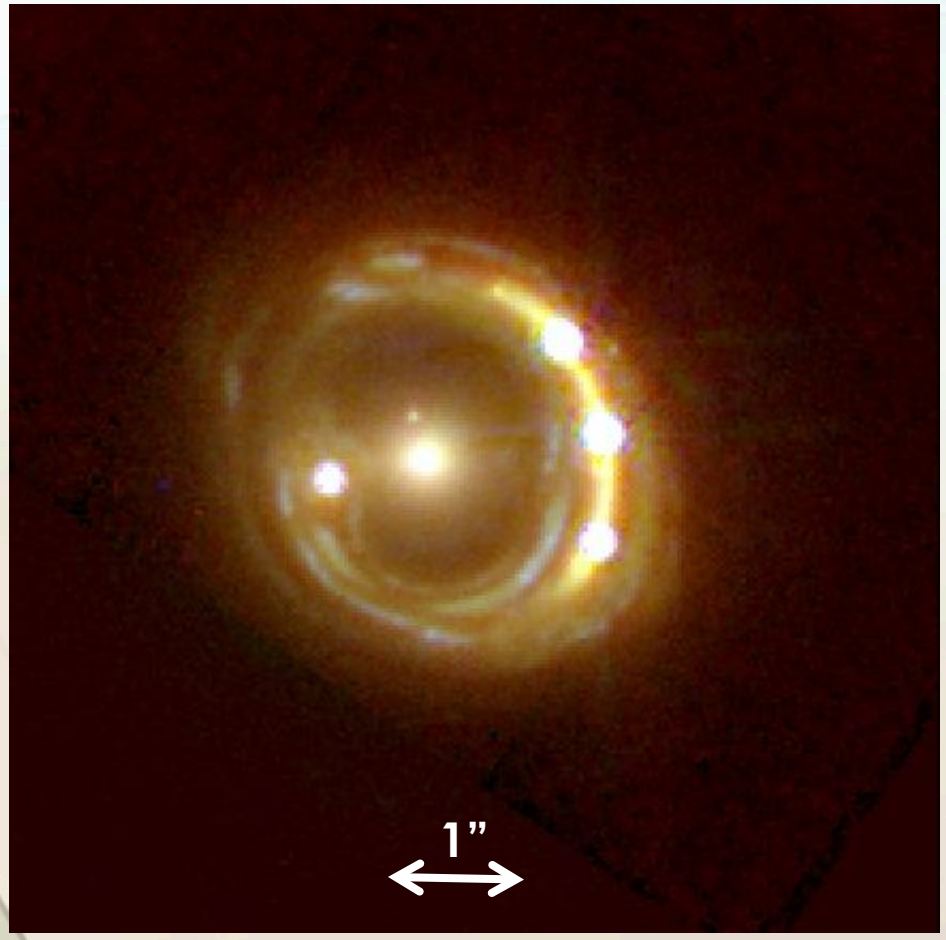

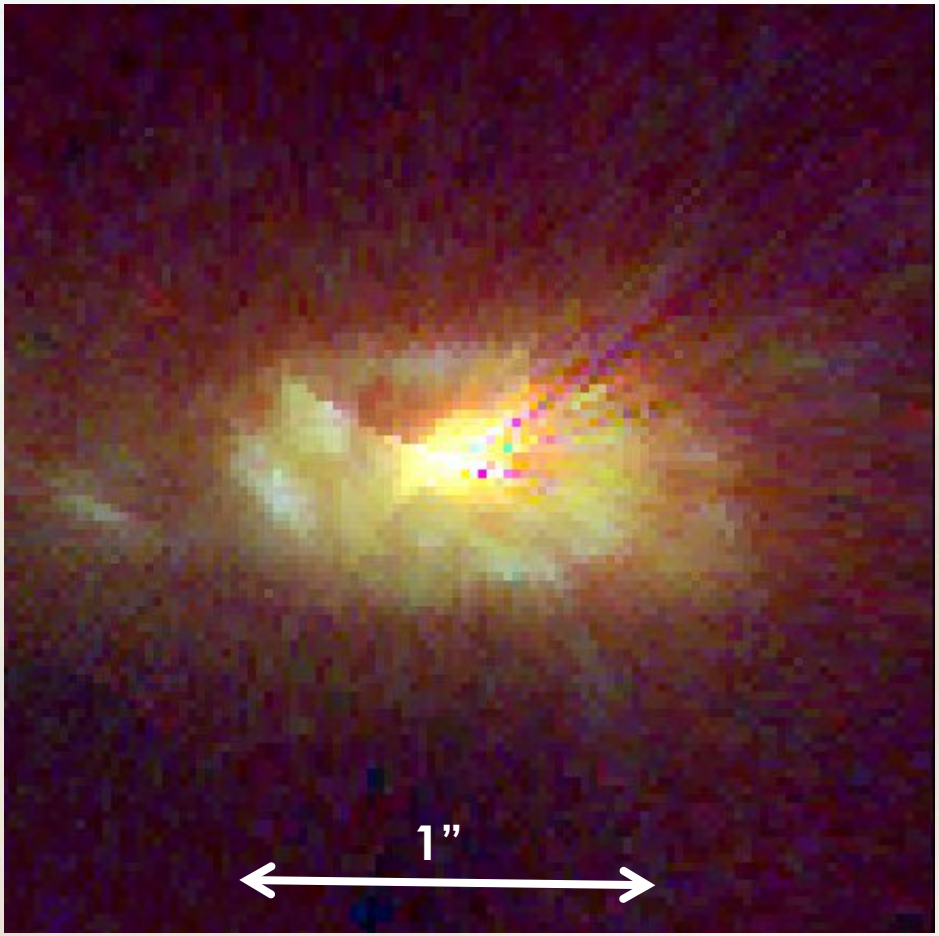

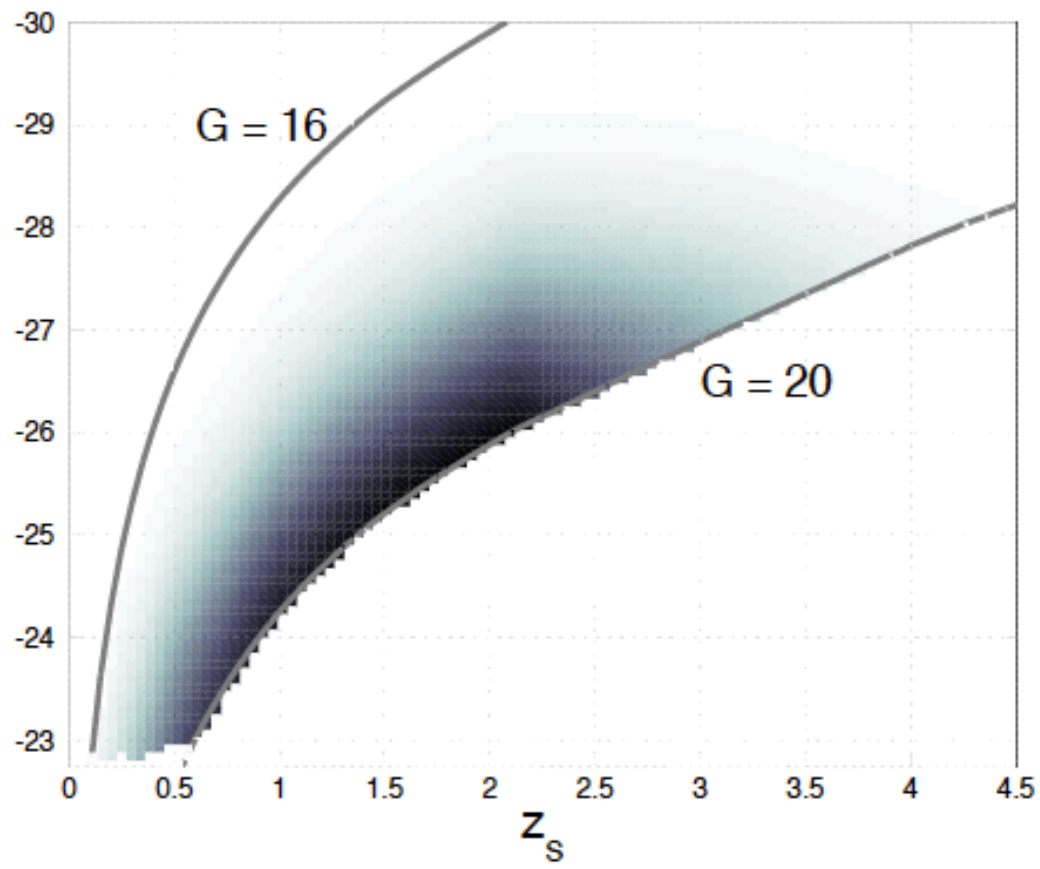

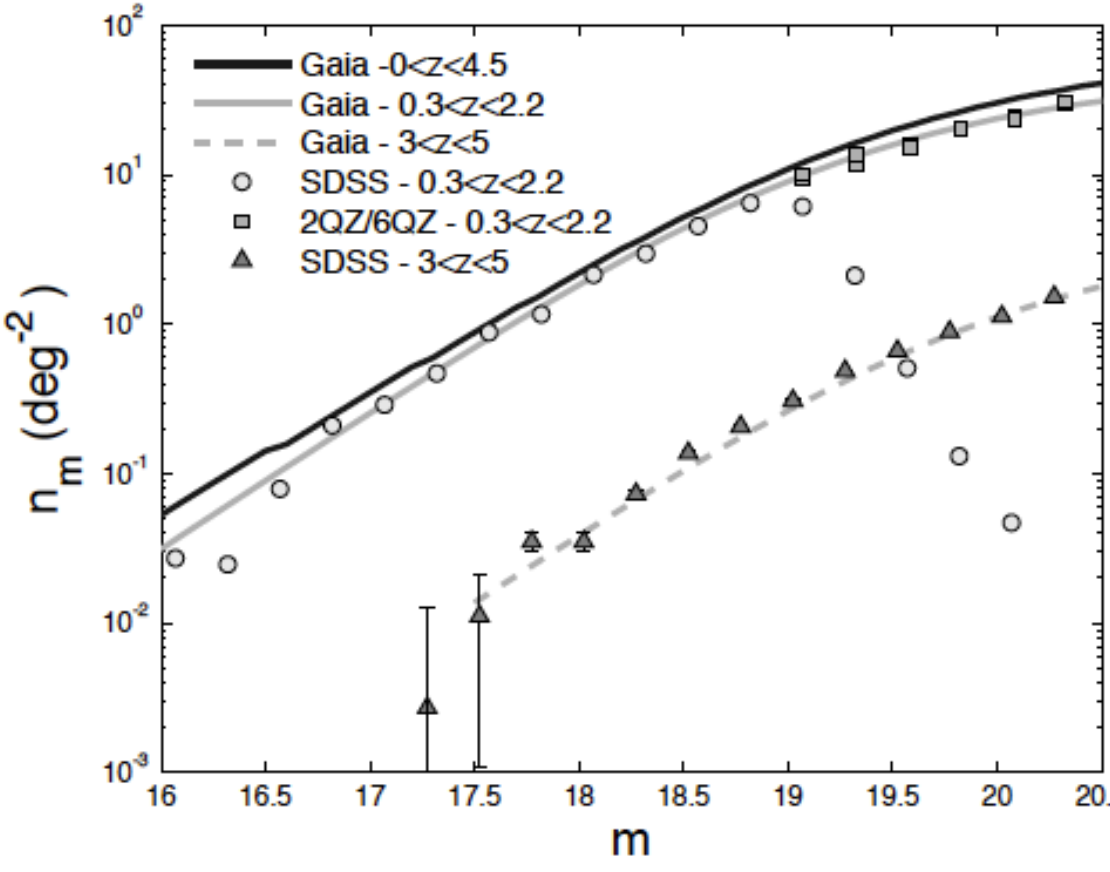

Left: Joint probability density $d_{obs}(z_s, M)$ for the Gaia sources, derived using the LF evolution model described in the text. Right: DN
on of the G-band magniude. We use a combined observational sample of the SDSS-DR3 and 2QZ/6QZ for magnitudes brighter (resp
) than $i \sim 19$, converted to G-band magnitudes and thus assuming the DNCF shape in G-band to be similar. We also show the fit
imation of the DNCF.

1. Comparison of the mean lensing optical depth and the expected number of detected multiply imaged sources for d
of the survey angular resolution corresponding to a perfect survey ($\theta_{mis} = 0$"), Gaia (0.2") and typical ground based obser
For each value of θ_{mis}, the table displays the average lensing optical depth $\langle\tau\rangle$ for both the SIS and SIE cases. In the latt
ction of lensing event as a function of the number i of lensed images is also displayed $\langle\tau_i\rangle / \langle\tau\rangle$. The bottom part of th
es the expected number of lenses in the survey, the total number as well as the number of events with a given number of
. For indication, we have reported the expected number of lensing events considering the population of sources found in M
nd Slezak 2007, assuming these sources have a similar distribution in the redshift-absolute magnitude diagram.

	N_{QSO}	$\theta_{mis} = 0$"		$\theta_{mis} = 0.2$"		$\theta_{mis} = 0.6$"	
				Early-type galaxies			
		SIS	SIE	SIS	SIE	SIS	SIE
	-	3.994×10^{-3}	3.747×10^{-3}	$\mathbf{3.917 \times 10^{-3}}$	$\mathbf{3.663 \times 10^{-3}}$	2.718×10^{-3}	2.431×1
$\langle\tau\rangle$	-	-	0.917	-	0.92	-	0.948
$\langle\tau\rangle$	-	-	1.15×10^{-3}	-	2.564×10^{-2}	-	4.614×1
$\langle\tau\rangle$	-	-	8.205×10^{-2}	-	5.25×10^{-2}	-	5.59×1
tudy	6.64465×10^5	2653	2490	**2602**	**2433**	1806	1615
ges	-	-	3	-	62	-	75
ges	-	-	204	-	134	-	9

Late-type galaxies							
		SIS	SIE	SIS	SIE	SIS	SIE
	-	1.278×10^{-3}	1.141×10^{-3}	$\mathbf{8.404 \times 10^{-4}}$	$\mathbf{6.815 \times 10^{-4}}$	-	-
$\langle\tau\rangle$	-	-	0.8413	-	0.92	-	-
$\langle\tau\rangle$	-	-	0.01206	-	0.07244	-	-
$\langle\tau\rangle$	-	-	0.1466	-	0.05192	-	-
udy	6.64465×10^5	849	758	**558**	**453**	-	-
es	-	-	9	-	33	-	-
es	-	-	111	-	24	-	-
All deflectors (early and late-type galaxies)							
		SIS	SIE	SIS	SIE	SIS	SIE
udy	6.64465×10^5	3502	3248	**3160**	**2886**	1806	161
ages	-	-	327	-	253	-	84
rd (2012)	$5.5 - 7 \times 10^5$						
(2007)	7.2×10^5						

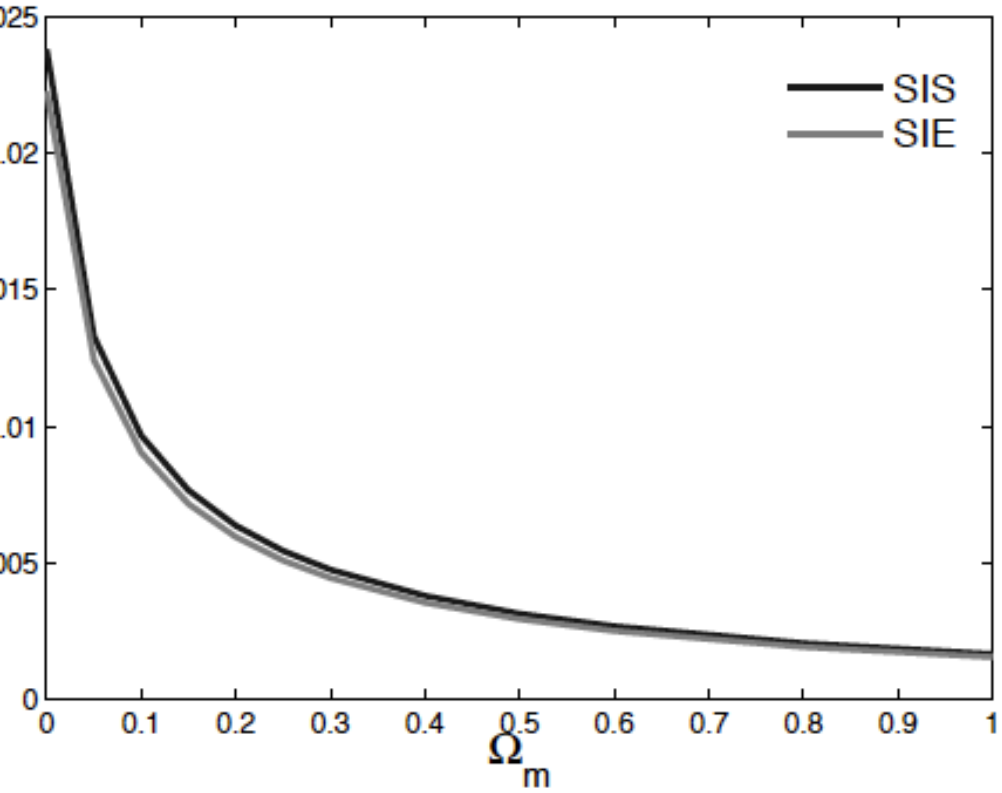

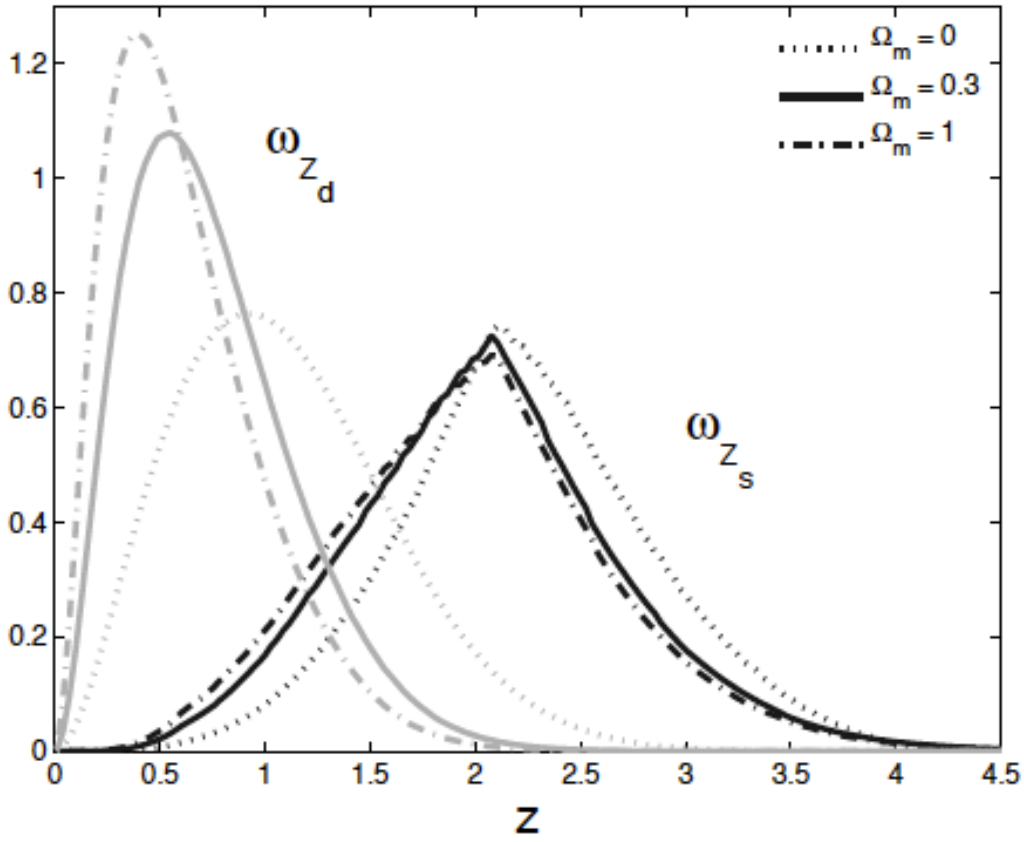

Left: average optical depth $\langle\tau\rangle$ (considering all deflector types) as a function of the cosmological matter density parameter Ω_m, m
flectors with the SIS and SIE models. *Right:* normalised redshift distributions ω_{z_s} and ω_{z_d} of the lensed sources and of the deflectors
ype galaxy population), for different values of $\Omega_m = 0, 0.3$ and 1. All simulations were produced for the case $\theta_{min} = 0.2$"

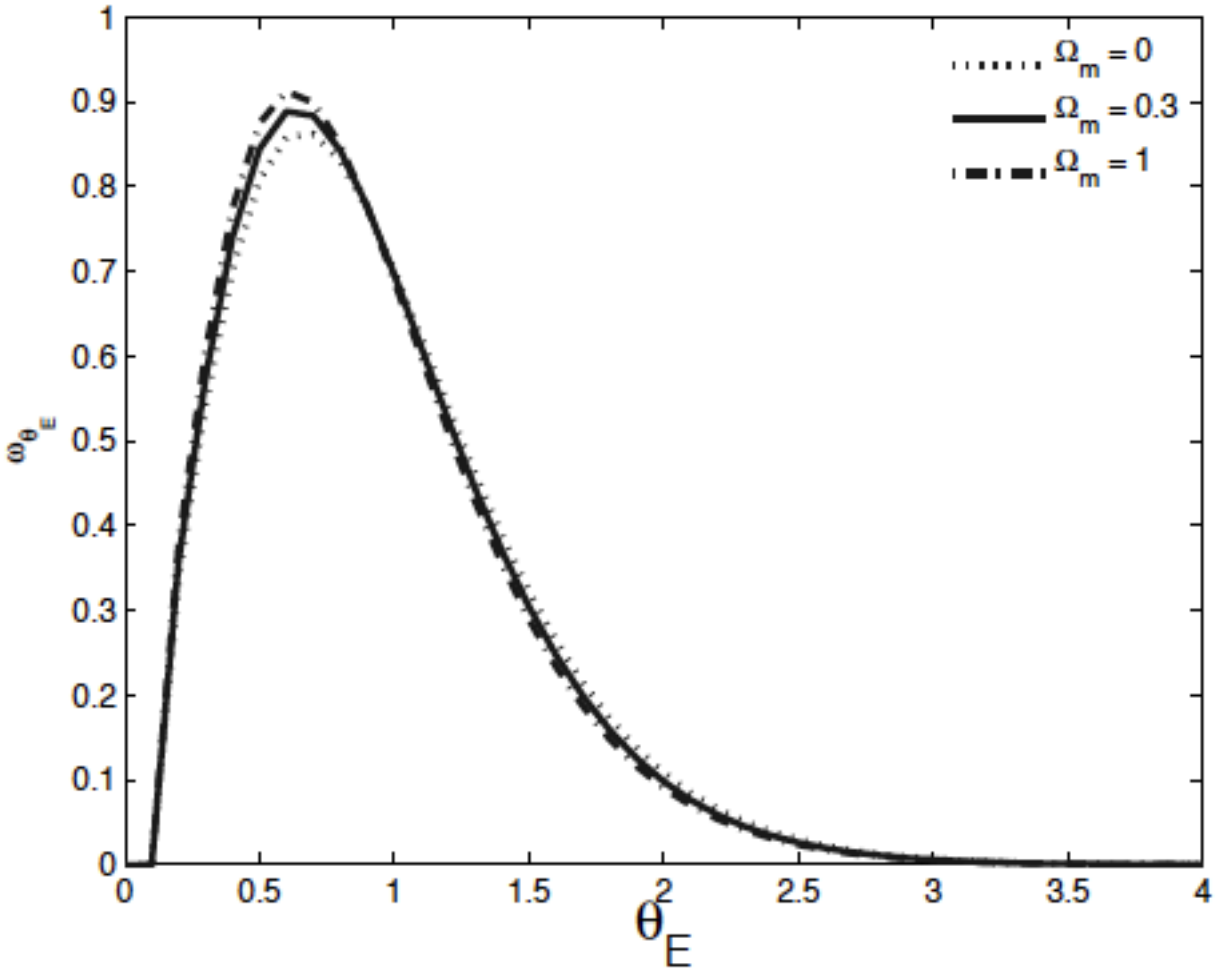

Fig. 8. Impact of the cosmological matter density parameter Ω_m on the normalised Einstein angular radius distribution $\omega_{\theta_E}(\theta_E)$ of the lensed sources. We have considered the deflectors to be modelled by SIS deflectors and an angular resolution $\theta_{min} = 0.2$" corresponding to the Gaia survey. θ_E are expressed in arcseconds.

616, L11 (2018)
/doi.org/10.1051/0004-6361/201833337
) 2018

Astronomy & Astrophysi

LETTER TO THE EDITOR

Gaia GraL: *Gaia* DR2 gravitational lens systems

I. New quadruply imaged quasar candidates around known quasars

A. Krone-Martins[1], L. Delchambre[2], O. Wertz[3], C. Ducourant[4], F. Mignard[5], R. Teixeira[6], J. Klüter[7], J.-F. Le Campion[4], L. Galluccio[5], J. Surdej[2], U. Bastian[7], J. Wambsganss[7], M. J. Graham[8], S. G. Djorgovski[8], and E. Slezak[5]

2. Relative astrometry and flux ratios of our newly discovered gravitationally lensed quasar candidates (GRAL113100–44195 122629–454209), and of a rediscovered system (GRAL203802–400815), from *Gaia* DR2 alone.

GRAL113100–441959			GRAL122629–454209			GRAL203802–400815		
$\Delta\alpha\cos(\delta)$ (″)	$\Delta\delta$ (″)	G-band flux ratio	$\Delta\alpha\cos(\delta)$ (″)	$\Delta\delta$ (″)	G-band flux ratio	$\Delta\alpha\cos(\delta)$ (″)	$\Delta\delta$ (″)	G flux
0.000(2)	0.000(1)	1.000(17)	0.000(1)	0.000(1)	1.000(6)	0.000(1)	0.000(1)	1.0
0.345(1)	−0.325(1)	0.947(10)	−3.066(1)	−1.705(1)	0.688(3)	1.515(1)	−0.029(1)	0.9
−1.282(1)	−0.425(1)	0.475(6)	0.065(1)	−5.453(1)	0.659(3)	−0.793(1)	1.676(1)	0.7
−0.343(1)	−1.511(1)	0.402(5)	4.986(2)	−2.092(2)	0.434(4)	1.379(2)	2.057(2)	0.5

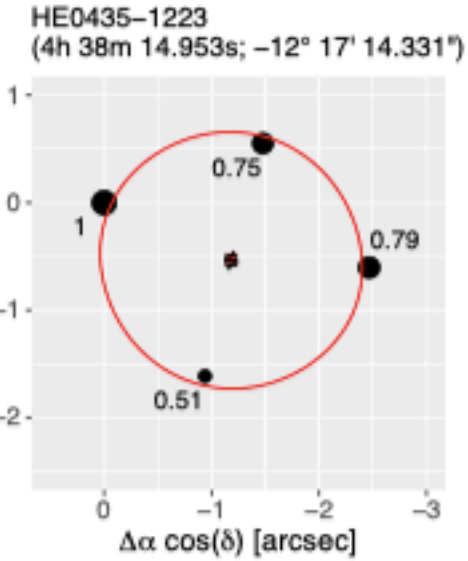

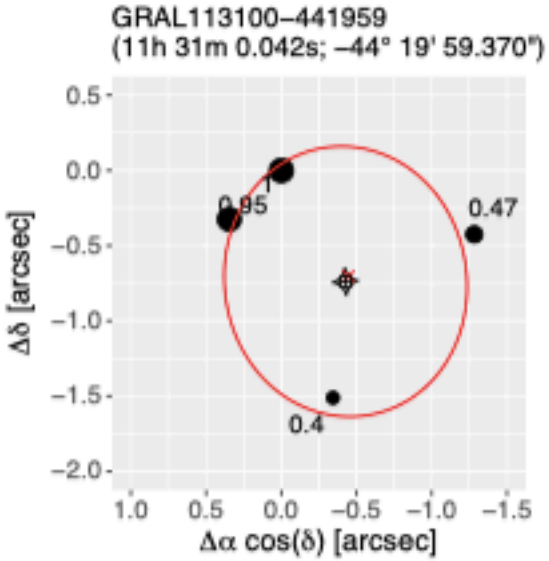

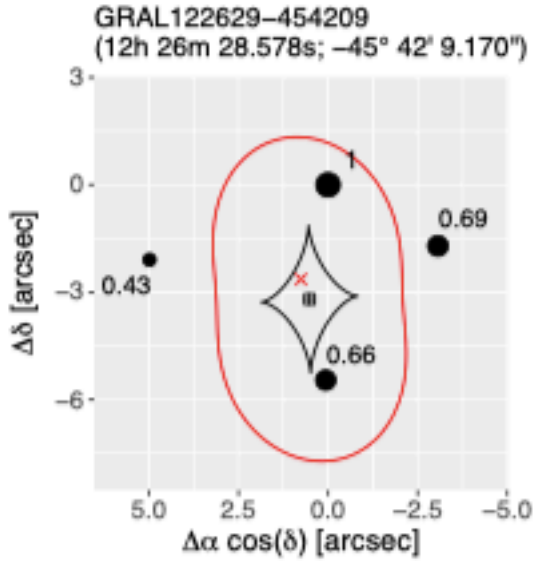

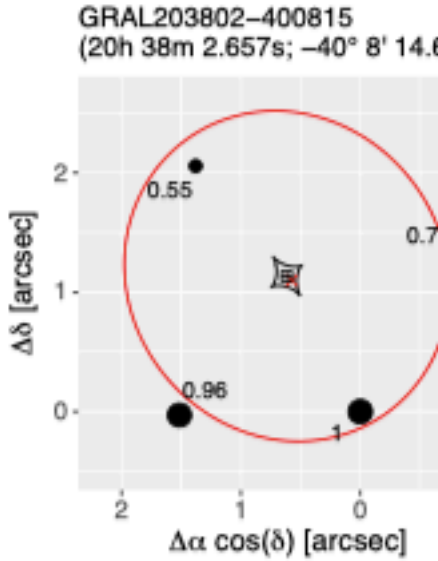

618, A56 (2018)
/doi.org/10.1051/0004-6361/201833480
) 2018

Astronomy & Astrophys

Gaia GraL: *Gaia* DR2 gravitational lens systems

II. The known multiply imaged quasars★

C. Ducourant[1], O. Wertz[2], A. Krone-Martins[3], R. Teixeira[4], J.-F. Le Campion[1], L. Galluccio[5], J. Klüter[6], L. Delchambre[7], J. Surdej[7], F. Mignard[5], J. Wambsganss[6,9], U. Bastian[6], M. J. Graham[8], S. G. Djorgovski[8], and E. Slezak[5]

Table 2. Relative astrometry for five known quadruply imaged quasars fully detected in the *Gaia* DR2.

Identifier	$\Delta\alpha\cos(\delta)$ (mas)	$\Delta\delta$ (mas)
HE0435-1223		
A	0.0 ± 0.16	0.0 ± 0.14
B	-1476.56 ± 0.19	552.94 ± 0.16
C	-2466.27 ± 0.21	-603.05 ± 0.16
D	-938.66 ± 0.30	-1614.43 ± 0.25
SDSS1004+4112		
A	0.00 ± 0.35	0.00 ± 0.52
B	1315.29 ± 0.36	3531.57 ± 0.49
C	-11039.10 ± 0.47	-4494.69 ± 0.68
D	-8403.23 ± 1.21	9701.47 ± 1.50
RXJ1131-1231		
A	588.68 ± 0.36	1118.89 ± 0.23
B	617.52 ± 0.39	2305.97 ± 0.25
C	0.0 ± 0.47	0.0 ± 0.30
D	-2522.23 ± 1.60	1993.80 ± 0.80
2MASS J1134-2103		
A	0.0 ± 0.11	0.0 ± 0.07
B	729.32 ± 0.11	1755.49 ± 0.07
C	-1947.39 ± 0.11	-772.70 ± 0.07
D	-1247.12 ± 0.28	1366.93 ± 0.20
WFI2033-4723		
A1	-2196.54 ± 0.33	1261.42 ± 0.34
A2	-1483.18 ± 0.26	1375.75 ± 0.30
B	0.0 ± 0.27	0.0 ± 0.24
C	-2113.84 ± 0.33	-277.84 ± 0.32

Notes. The image references have been chosen to match those reported either in https://www.cfa.harvard.edu/castles/ or in their reference papers. They are not necessarily the brightest images in the *Gaia* *G*-band.

Table 3. SIEg lens model parameters derived for HE0435-1223.

Parameters	HST	*Gaia*
$\theta_{\rm E}$ ($''$)	1.2 ± 0.003	1.2 ± 0.002
q	0.93 ± 0.03	0.9210 ± 0.01
θ_q ($^\circ$)	-69.4 ± 3.8	-69.5 ± 0.8
γ	0.087 ± 0.005	0.088 ± 0.002
θ_γ ($^\circ$)	15.7 ± 0.9	15.9 ± 0.1
β_x (mas)	-1182.0 ± 1.6	-1181.7 ± 0.1
β_y (mas)	-521.4 ± 2.1	-521.6 ± 0.1
$x_{\rm G}$ (mas)	-1176.7 ± 1.5	-1176.6 ± 0.3
$y_{\rm G}$ (mas)	-554.2 ± 3.7	-553.6 ± 1.2

Note. The reported values are medians within 1σ error bars.

622, A165 (2019)
doi.org/10.1051/0004-6361/201833802
2019

Astronomy & Astrophys

Gaia GraL: *Gaia* DR2 Gravitational Lens Systems

III. A systematic blind search for new lensed systems★

elchambre[1], A. Krone-Martins[2], O. Wertz[3], C. Ducourant[4], L. Galluccio[5], J. Klüter[6], F. Mignard[5], R. Teixe
S. G. Djorgovski[8], D. Stern[9], M. J. Graham[8], J. Surdej[1], U. Bastian[6], J. Wambsganss[6,10],
J.-F. Le Campion[4], and E. Slezak[5]

[1] Institut d'Astrophysique et de Géophysique, Université de Liège, 19c, Allée du 6 Août, 4000 Liège, Belgium
e-mail: ldelchambre@uliege.be

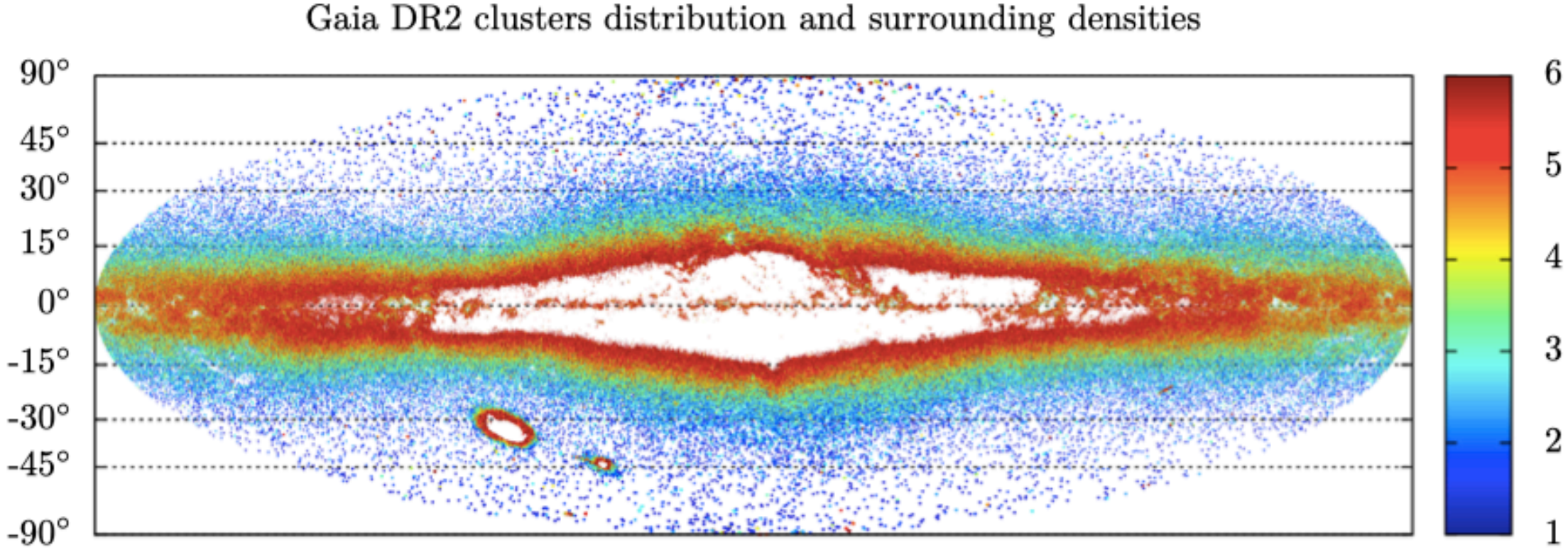

Distribution of the 2 129 659 clusters of objects extracted from the *Gaia* DR2 catalogue. They are composed of three and four ima
e soft astrometric test (see Sect. 2) that have a maximum angular separation between components that is smaller than 6″, that have a
nces in G magnitudes of <4 mag, and that are found in regions of the celestial sphere where the mean field density is lower than
deg^{-2}. Lower density regions near the galactic centre can be explained by the filtering occurring in the on-board processing in
memory from saturating in such very dense regions of the sky (Gaia Collaboration 2016).

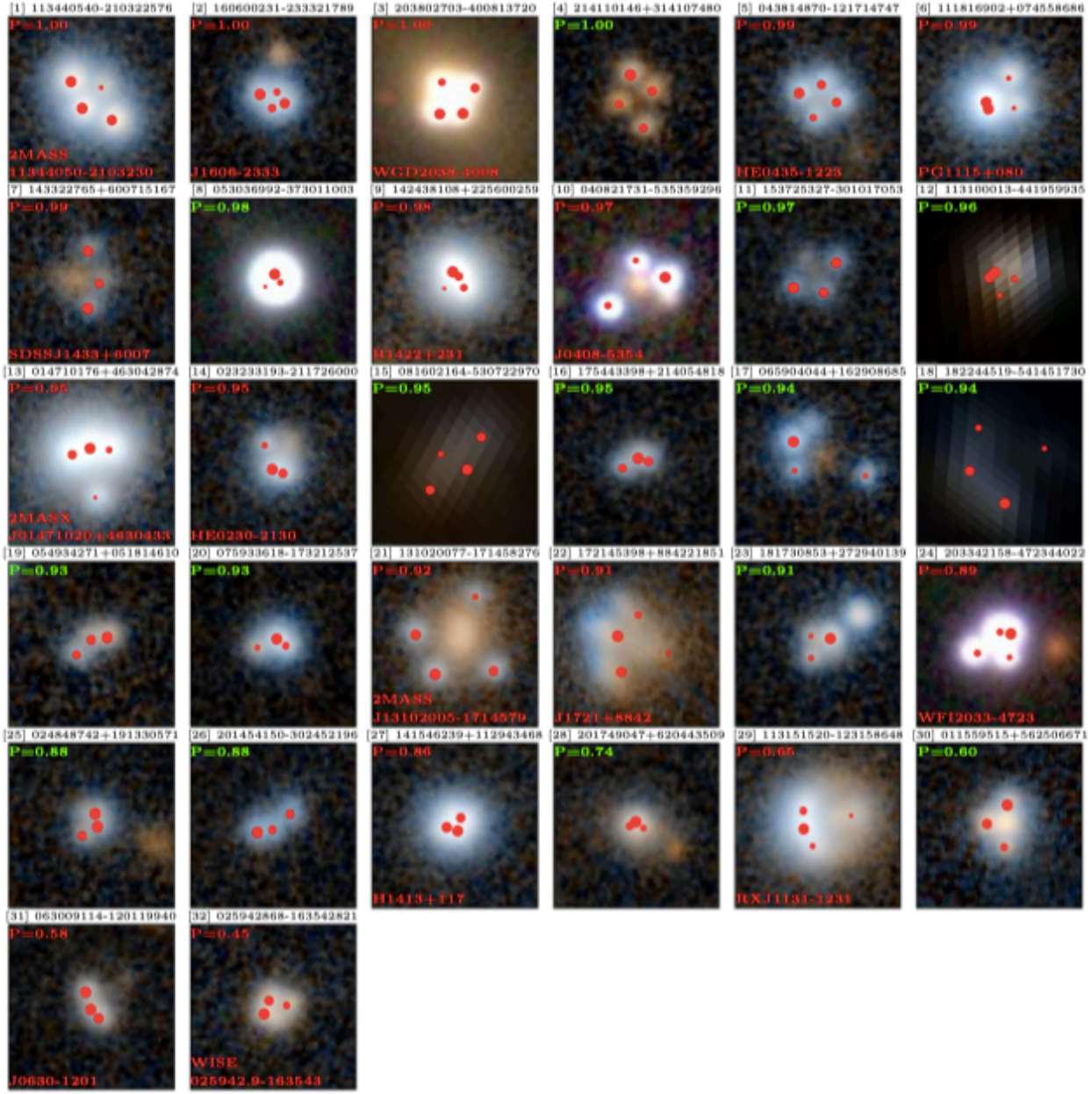

Fig. 4. Finding charts of the 17 known GLs and 15 GL candidates contained in our catalogue of clusters (Appendix B). They are ordered according to their ERT probabilities (upper left corner of each subplot). The common name of the known lenses is labelled in red in the lower left corner of each subplot, while the candidates we propose have their probabilities written in green fonts. Images [1], [2], [4–7], [9], [11], [13], [14], [16], [17], [19–23], [25–32] come from the Pan-STARRS survey (Chambers et al. 2016); images [12], [15], [18] come from the Digitized Sky Survey II (Lasker et al. 1996); and images [3], [8], [10], [24] come from the DES (Dark Energy Survey Collaboration et al. 2016). All images were collected from the ALADIN sky atlas (Bonnarel et al. 2000) in a field of view of $10.8'' \times 10.8''$ centred around the mean coordinates of the GL where east is to the left and north is up. Points are scaled according to the relative flux of the components with respect to the brightest image of each configuration.

Table 3. List of GL candidates.

Num.	Candidate identifier	N_{img}	Right ascension (°)	Declination (°)	Size (mas)	Field density (obj. deg^{-2})	ΔG (mag)	$\Delta(G_{BP} - G_{RP})$ (mag)	ERT prob.
[4]	214110146+314107480	4	325.292262	31.685426	3602	27 502	0.67		1.00
[8]	053036992–373011003	3	82.654147	–37.503067	1036	27 502	2.99		0.98
[11]	153725327–301017053	3	234.355552	–30.171385	3286	45 837	0.22	0.63(2)	0.97
[12]	113100013–441959935	4	172.750041	–44.333297	1631	36 669	0.99	0.02(2)	0.96
[15]	081602164–530722970	4	124.009037	–53.123042	4823	27 502	0.87	0.34(3)	0.95
[16]	175443398+214054818	3	268.680823	21.681869	1755	18 335	0.45		0.95
[17]	065904044+162908685	3	104.766823	16.485772	5249	36 669	1.47	0.14(2)	0.94
[18]	182244519–541451730	4	275.685519	–54.247701	5256	27 502	1.22	0.11(4)	0.94
[19]	054934271+051814610	3	87.392794	5.304042	2298	45 837	0.43		0.93
[20]	075933618–173212537	3	119.890101	–17.536806	1860	55 004	1.23		0.93
[23]	181730853+272940139	3	274.378545	27.494468	1796	36 669	1.79		0.91
[25]	024848742+191330571	3	42.203097	19.225140	1677	13 751	0.30	0.06(2)	0.88
[26]	201454150–302452196	3	303.725615	–30.414491	2465	13 751	0.48	0.32(2)	0.88
[28]	201749047+620443509	3	304.454360	62.078774	916	36 669	0.99		0.74
[30]	011559515+562506671	3	18.997963	56.418524	2756	45 837	0.70		0.60

Notes. The finding charts depicting all of these candidates are given in Fig. 4. The numbers in parentheses in Col. $\Delta(G_{BP} - G_{RP})$ correspond to the number of images that were used in the computation of the maximum absolute difference in colour.

A&A 628, A17 (2019)
https://doi.org/10.1051/0004-6361/201834573

Astronomy & Astrophysics

Gaia GraL: *Gaia* DR2 gravitational lens systems

IV. Keck/LRIS spectroscopic confirmation of GRAL 113100−441959 and model prediction of time delays

O. Wertz[1], D. Stern[2], A. Krone-Martins[3], L. Delchambre[4], C. Ducourant[5], U. Gråe Jørgensen[12], M. Dominik[13], M. Burgdorf[14], J. Surdej[4], F. Mignard[6], R. Teixeira[7], L. Galluccio[6], J. Klüter[8], S. G. Djorgovski[9], M. J. Graham[9], U. Bastian[8], J. Wambsganss[8,10], C. Boehm[11], J.-F. LeCampion[5], and E. Slezak[6]

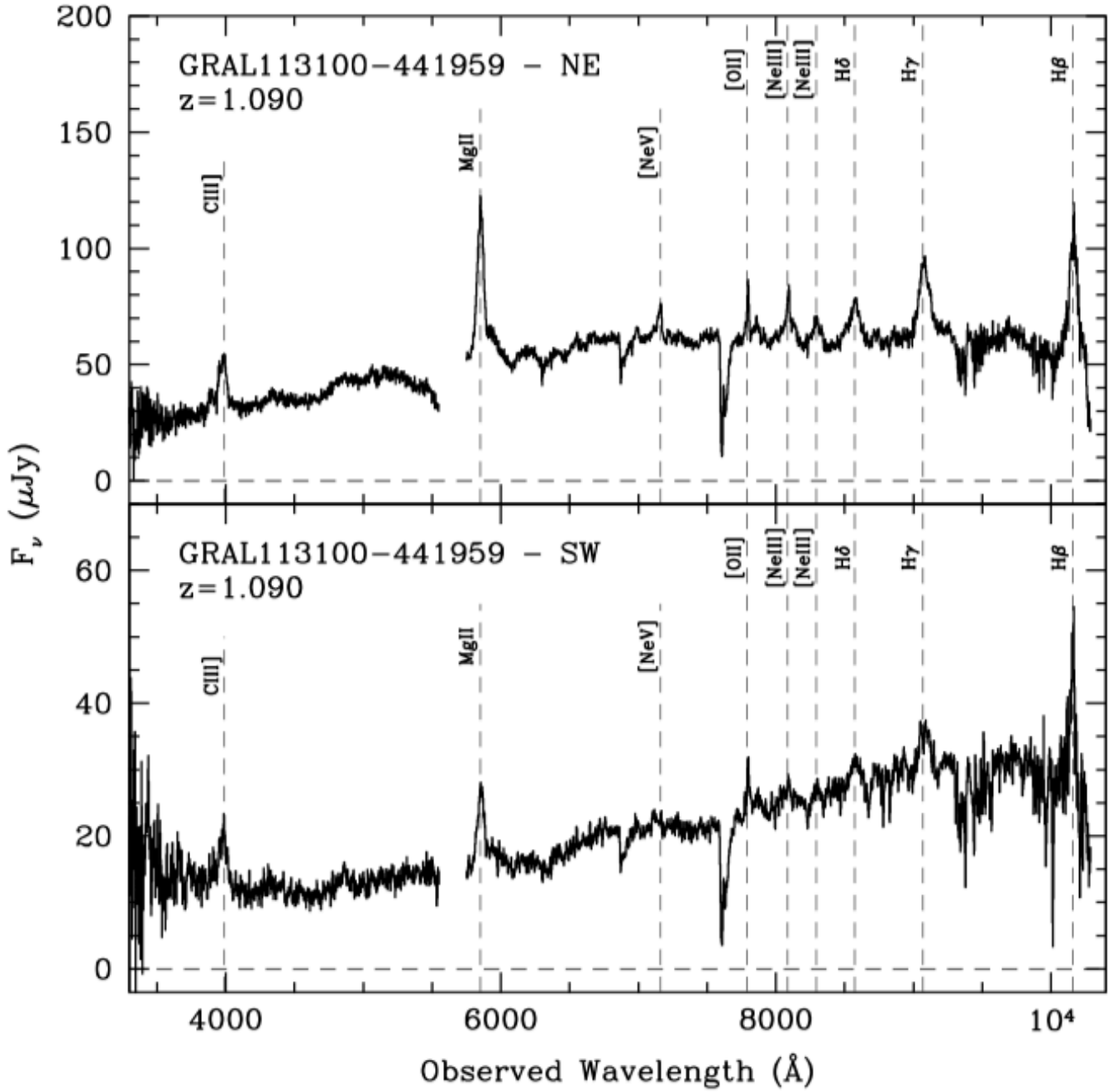

Fig. 1. Keck/LRIS spectra of images (A+B) and (C+D) at position angle 60°. Dashed lines identify emission lines used to confirm the lensing nature of GRAL 113100–441959.

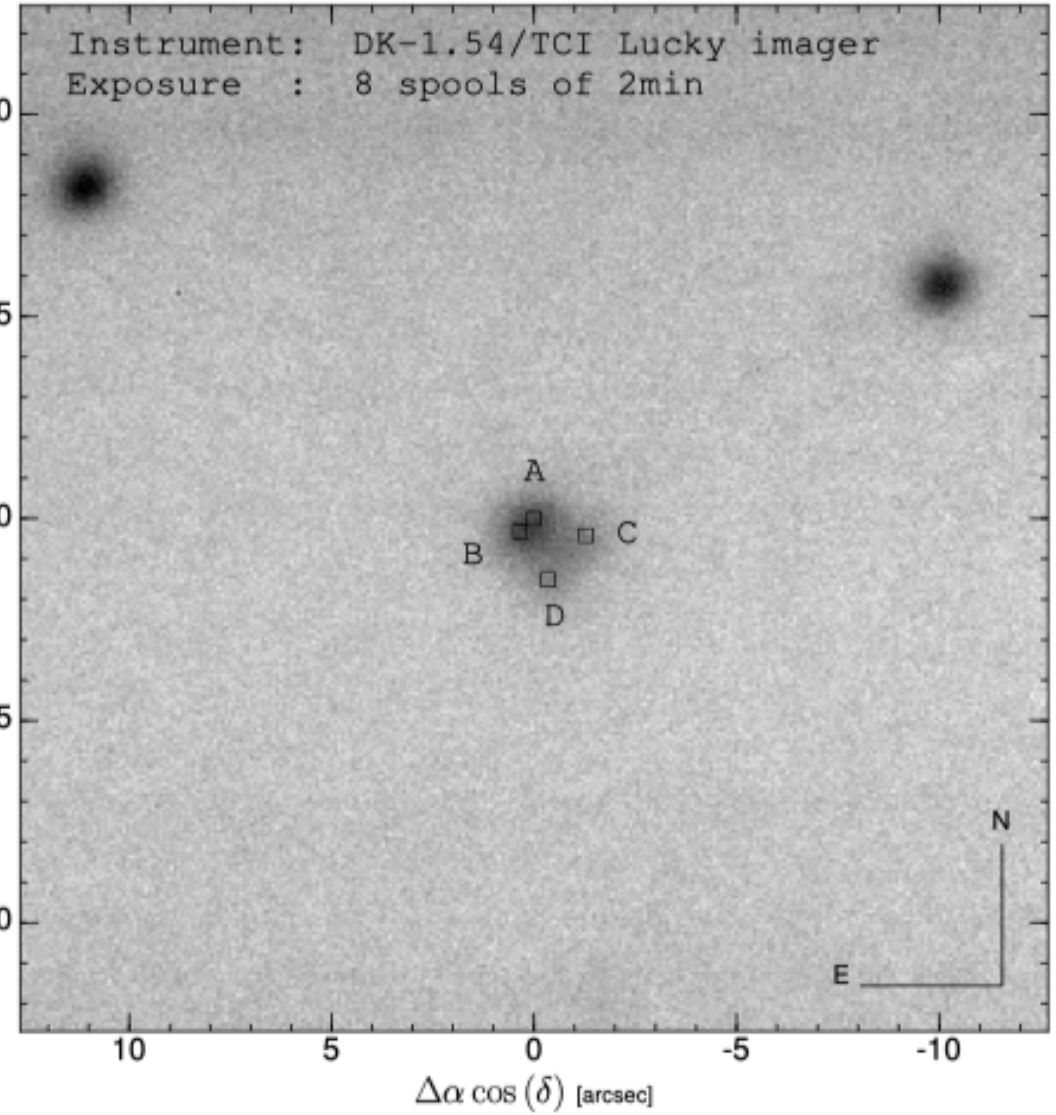

2. First direct imaging of GRAL 113100–441959 obtained with DK-1.54/TCI Lucky imager during the night of UT 2018 July 31 ite observer: Martin Burgdorf). The black squares locate the lensed ed positions as reported in the *Gaia* DR2.

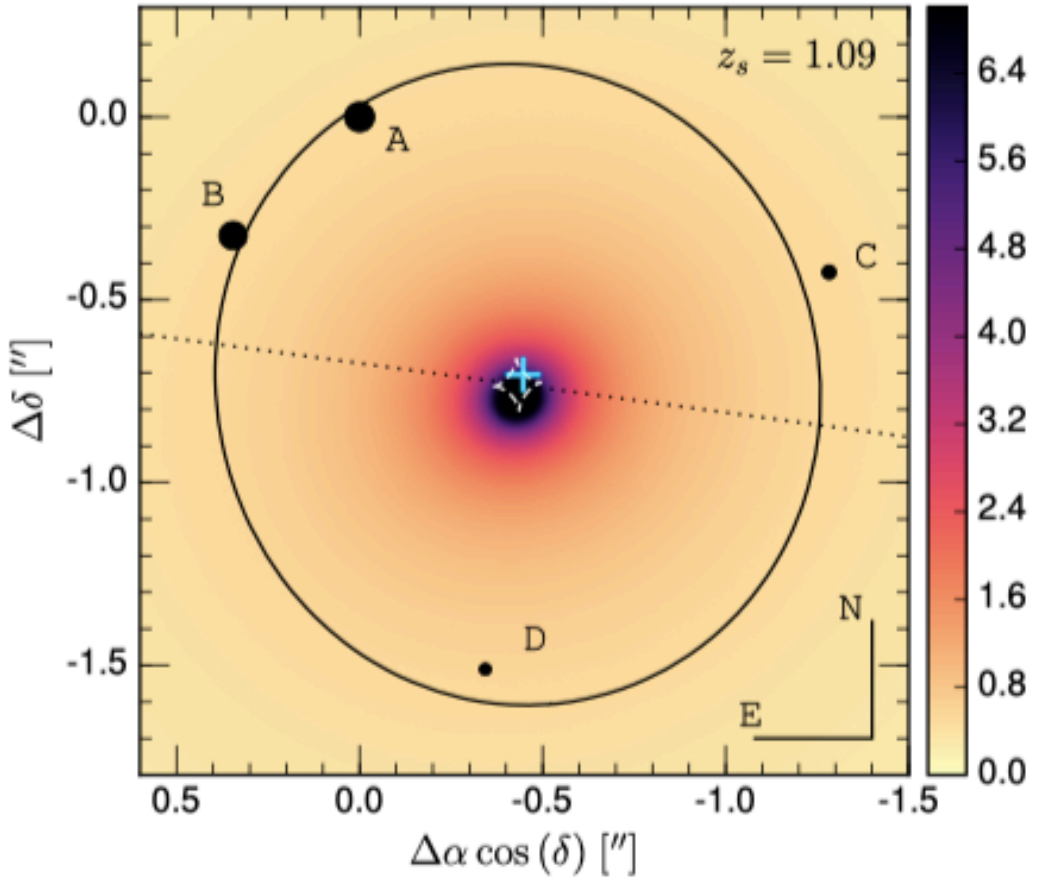

Fig. 5. GRAL 113100–441959 image configuration. The black locate the image positions, and their size mimics the associated as reported in the *Gaia* DR2. The solid line represents the tange critical line, the diamond-shaped dashed line represents the corresp ing caustic line, and the dotted line defines the direction of the ext shear. Finally, the color map shows how the surface mass density distributed.

The 4m International Liquid Mirror Telesco

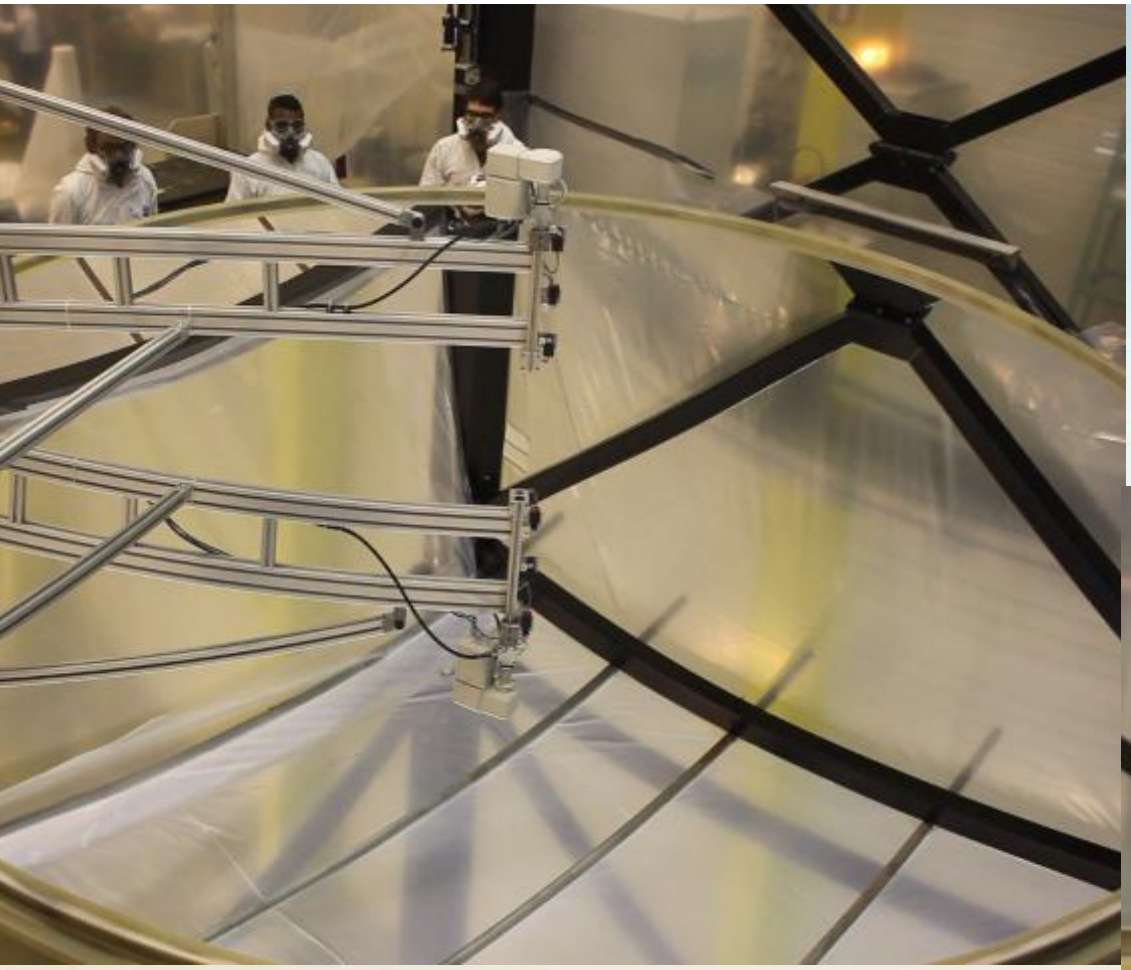

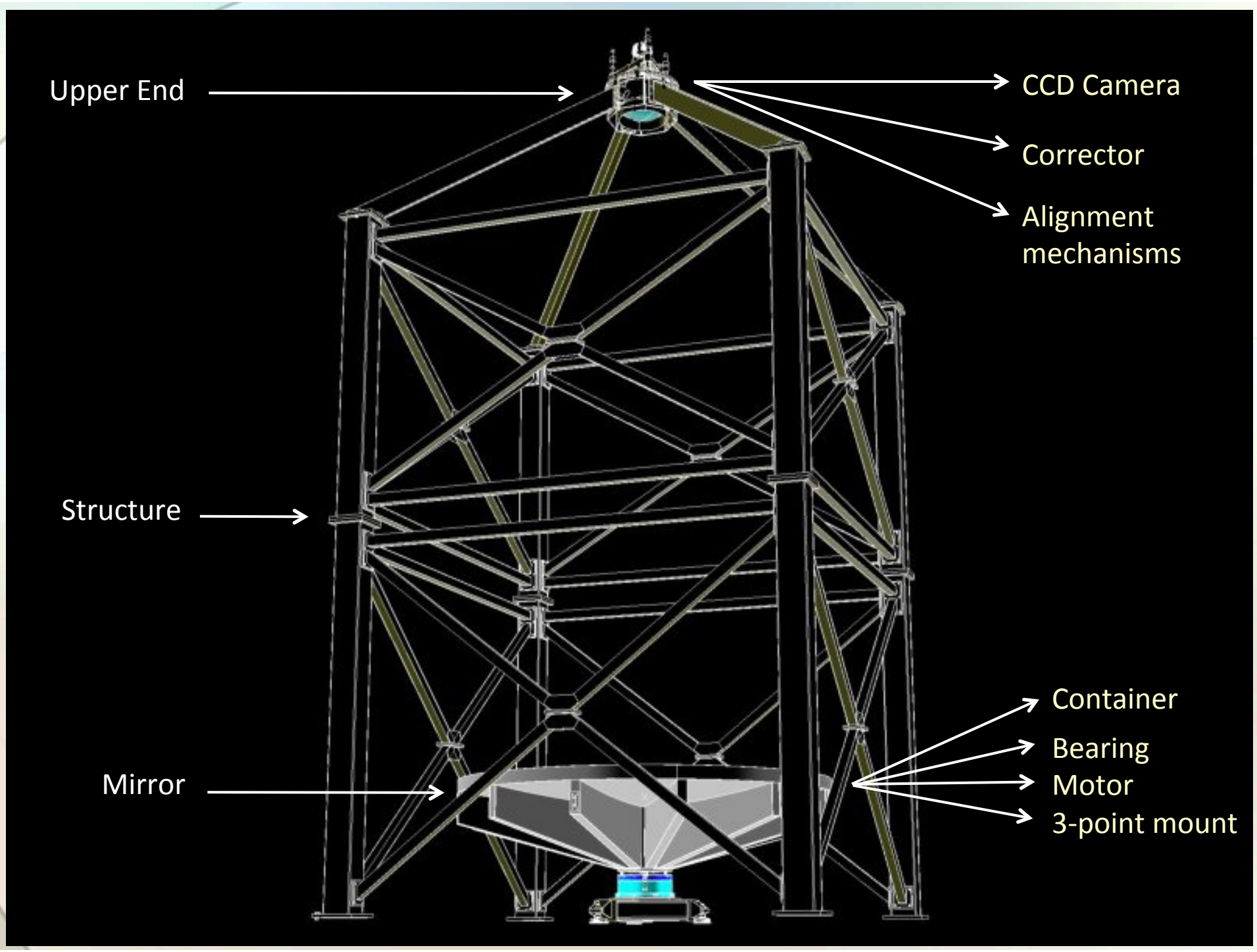
Upper End
CCD Camera
Corrector
Alignment mechanisms
Structure
Container
Bearing
Motor
3-point mount
Mirror

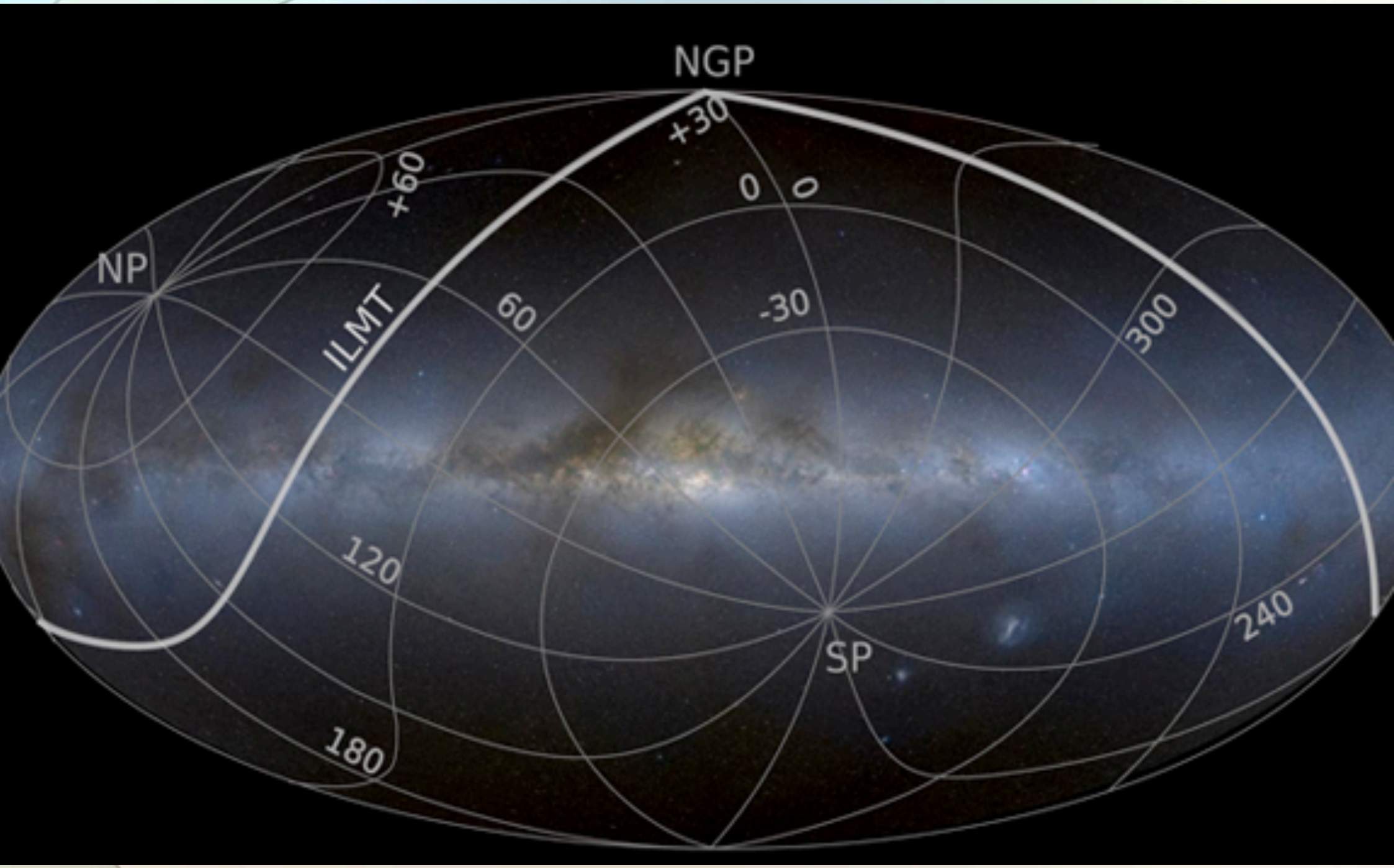
NGP
+30
+60
0
0
NP
ILMT
60
-30
300
120
240
SP
180

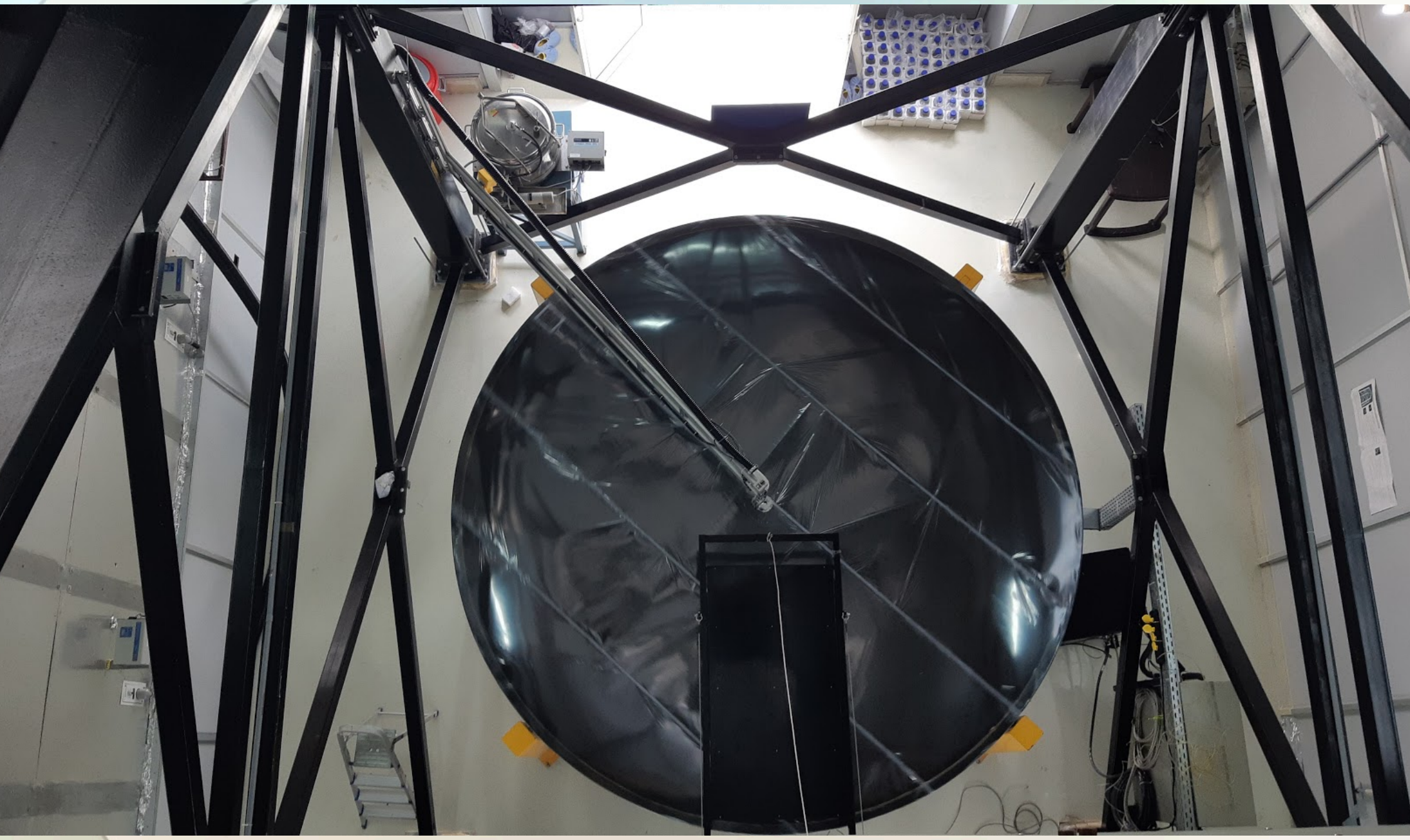


VLC Fichier Édition Vue Lecture Audio Vidéo Sous-titres Fenêtre Aide
Jeu. 06:34 Jean Surdej
172.20.2.37_01_20190419190553876_1.mp4
04/19/2019 19:39:5
AMOS
ADVANCED MECHANICAL AND OPTICAL SYSTEMS S.A.
LIÈGE
université
Cam-13-LLMT
02:37

SIS + γ